UNCLASSIFIED

AD 407 685

DEFENSE DOCUMENTATION CENTER

FOR

SCIENTIFIC AND TECHNICAL INFORMATION

CAMERON STATION, ALEXANDRIA, VIRGINIA

407 685

$63-4-1$

$\boxed{16}$

FINAL REPORT

RESEARCH ON THE APPLICATION OF BINARY GAS MIXTURES TO LOW TEMPERATURE COOLING SYSTEMS

May 20, 1963

RECONNAISSANCE LABORATORY
AERONAUTICAL SYSTEMS DIVISION
AIR FORCE SYSTEMS COMMAND
WRIGHT-PATTERSON AIR FORCE BASE, OHIO

Project No. 4077, Task No. 407703

JUN 9 1963

TISIA A

FOREWORD

This final report was prepared by the AiResearch Manufacturing Company of Los Angeles, a division of The Garrett Corporation, under contract to the Reconnaissance Laboratory, Aeronautical Systems Division, Wright-Patterson Air Force Base, Ohio. The report summarizes the work performed for ADS Contract AF33(657)-8672, the purpose of which was to investigate the applicability of binary gas mixtures as cryogenic refrigerants. Mr. R. B. Cunningham was project engineer for the Reconnaissance Laboratory.

This report was prepared by C. W. Browning, an engineer in the Preliminary Design Department of AiResearch Manufacturing Company. Mr. Browning functioned as the principal investigator throughout the performance of the contract.

Other personnel who made contributions to this report are F. E. Maddocks and G. A. Burgess. Mr. Maddocks was the program manager. Mr. Burgess reviewed the report prior to its submittal to the Reconnaissance Laboratory.

Acknowledgement is given to Dr. J. M. Lenoir, Professor of Chemical Engineering, University of Southern California, and D. G. Morgan of AiResearch. Dr. Lenoir acted as consultant throughout the program and his contributions were important to the success of the program. Mr. Morgan assembled the apparatus.

This is the final report under Contract AF33(657)-8672. The contractor's report number is SS-881-R.

ABSTRACT

This report describes an investigation to determine the utility of several binary gas mixtures as cryogenic refrigerants. The literature was searched for the existence of data required for evaluation of the applicability of the selected mixtures. Since the fragmentary nature of the existing data on the binary mixtures of interest was confirmed by the literature search, a test program was initiated.

An experimental apparatus was designed and fabricated which permitted direct determinations of the phase boundaries of the selected cryogenic gas mixtures. Although no attempt was made in the experiments conducted under the study to obtain this type of data, this apparatus is also suitable for PVT data determinations. The apparatus is based on the dew point and bubble point method. The general principle of this method and the experimental apparatus and procedure for its operation are described in detail in this report.

Experimental data were obtained for the binary systems of neon-argon and nitrogen-argon. These data consist of solid vapor, dew point, bubble point, and the three-phase boundaries at a fixed composition. Also, dew point curves were determined for three additional neon-argon mixtures.

The possible application of the selected mixtures is discussed. In addition, the general problem areas and possible advantages of utilizing binary mixtures as cryogenic refrigerants are analyzed.

ASD-TDR-63-339

TABLE OF CONTENTS

TABLE OF CONTENTS (Continued)

LIST OF FIGURES

SECTION 1

INTRODUCTION

This report summarizes the engineering activities of the AiResearch Manufacturing Company, a Division of The Garrett Corporation, on ASD Contract AF33(657)-8672. The purpose of this contract was to investigate several binary gas mixtures for possible use as cryogenic refrigerants.

At present, closed-cycle cryogenic refrigeration systems are limited to the use of pure elementary gases as refrigerants. In the case of vapor-liquid cycles, the refrigeration temperatures achievable are limited to a narrow range near the normal boiling point of the gas used, with the triple and critical temperatures as the absolute limits.

The principal use of cryogenic refrigerators in aerospace applications is for cooling solid-state electronic devices such as infrared sensors, masers, lasers, and microswitching elements. These devices in general, require very low refrigeration capacities, which, coupled with the high premium placed on weight and volume for space applications, result in strong emphasis on miniaturization techniques. Miniaturization gives rise to design and fabrication problems which can be reduced by using binary gas mixtures as the refrigerant.

From the data obtained in the course of the experimental investigations performed under this contract, it appears that binary mixtures offer several possible advantages as cryogenic refrigerants. In fact, it may prove possible to tailor various mixtures to the capabilities of the mechanical components of a given system, thus allowing optimum system configurations with increased efficiency and reduced weight. This study, however, can only be considered as an initial probe into the wide applications which could arise from a more complete knowledge of the properties and behavior of specific mixtures.

SECTION 2

SUMMARY

The initial phase of this program consisted of a literature survey, the results of which are given in Section 3 of this report. Because of the scarcity of published data, the design, fabrication, and calibration of an experimental apparatus to obtain the required data were undertaken as the second phase of the program. This apparatus is described in Section 5. The third phase of this program consisted of the experimental investigations. The methods utilized are described in Section 4. The data obtained are presented and evaluated in Section 6. Section 7 consists of a discussion of the applicability of binary gases to cryogenic refrigeration systems. Section 8 presents conclusions and recommendations.

The significant experimental findings are as follows: In the binary system of neon-argon, no measurable three-phase point depressions were observed at moderate pressures. At temperatures near the triple point of argon, neon is only slightly soluble in the liquid phase. The system of neon-argon does not appear applicable to vapor-liquid cycles because of the large difference between the dew and bubble point pressures at a given temperature. However, the application of neon-argon and similar mixtures to gas cycles appears very promising.

A mixture of 43.17 percent nitrogen in argon was investigated experimentally. In this case, a $15^\circ K$ three-phase point depression was observed. This mixture could easily be used in vapor-liquid cycles, operating well below the triple point of pure argon.

SECTION 3

LITERATURE SEARCH

The literature was surveyed for two basic reasons: to determine the availability of existing phase equilibrium data on the selected binary mixtures, and to evaluate the experimental methods and apparatus that have been used for investigation of phase equilibria at low temperatures. The binary mixtures initially selected for investigation are given on Page 49.

AVAILABLE DATA

The scarcity of published phase equilibria data is attributed to infrequent applications entailing mixtures of cryogenic gases and to the comparative lack of interest in cryogenics before the last two decades. A contributing factor to the paucity of data is certainly the experimental difficulties that are incurred in bringing a mixture to exact equilibrium under well-defined conditions of temperature and pressure (1). Compared with measurements that can be carried out near room temperature, measurements at cryogenic temperatures entail additional insulation problems, resulting in greater complexity of apparatus and procedures.

The system of hydrogen and nitrogen has been investigated. However, the low-pressure region, which is of particular importance for this study, has been neglected. A complete survey of the existing data on this system is given in Technical Note 110 published by the National Bureau of Standards (2). This reference also contains a valuable bibliography.

Hala (3) gives a list of references on vapor-liquid data sources. According to this list, the neon-hydrogen system has been investigated by Brown (4). However, Brown's data could not be located; they were evidently given in an oral presentation but not published.

EXPERIMENTAL METHODS

The literature describing experimental determinations of phase equilibria at low temperatures is limited. Ruhemann (1) presents a brief description of the experimental methods that have been used to obtain such data as well as a summary of low-temperature phase equilibrium data that had been obtained up

3

to 1945. Aston and Fink (5) have published an excellent review of low-tempera-
ture techniques in physicochemical research. Katz and Rzasa (6) have prepared
a bibliography with complete references on the classic investigations carried
out before 1910 on liquid-vapor phase equilibria and critical phenomena.
Bloomer and Parent (7) present an excellent survey of the literature on exper-
imental techniques utilized through 1951. Hala (3) presents a detailed
description of the common equilibrium apparatuses and gives a reference list
of data obtained through 1957. Since 1957, little additional information
has been published.

Phase equilibria data have been obtained by several methods. Both
Ruhemann (1) and Edmister (8) have classified the methods in terms of the
apparatus used. Their classifications are similar, differing mainly in
terminology. Ruhemann classified the general methods as follows:

1.   Dew and bubble point method

2.   Static or batch method

3.   Flow method

4.   Circulation method

DESCRIPTION OF METHODS

Dew and Bubble Point Method

The dew and bubble point method consists in charging known amounts of
gas mixture into an equilibrium cell of known volume at a fixed temperature.
The pressure within the cell is increased by successive additions of gas
mixture while the temperature is maintained constant. Eventually a pressure
is reached at which a new phase will appear. Thus, one point on a phase
boundary is determined.

Numerous investigators have successfully used this method for vapor-liquid
equilibria studies (6 to 22). The dew and bubble point method can be used to
obtain PVT data in addition to establishing the liquid-vapor phase boundaries.
The necessary procedures and equipment have been presented by Bloomer and
Parent (7).

4

Kurata and Kohn (9) have shown how the general principle of the dew and bubble point method can be expanded into a very versatile experimental method. They list the following types of data that can be obtained with their apparatus:

1. Solid-liquid-vapor equilibria

2. Vapor-liquid equilibria

3. PVT measurements

4. Solid-liquid equilibria

5. Solid-vapor equilibria

6. Partial miscibility in binary systems

7. Viscosity relationships

8. Solid solubilities

Of the items listed above, 1, 2, and 3 are of primary importance in determining the applicability of a given binary mixture to closed-cycle cryogenic refrigeration.

The basic dew and bubble point method and the modified method of Kurata and Kohn (9) are more fully discussed in Section 4.

Static or Batch Method

In the static or batch method, a fixed quantity of a mixture is held in a cell at constant temperature until equilibrium is established. Samples of the separate phases are then withdrawn for analysis. Baly (23) was the first to use this method at low temperatures for the oxygen-nitrogen system. He was followed by Verschoyle (24 and 25), who investigated hydrogen-nitrogen-carbon monoxide mixtures; and Fedoritenko and Ruhemann (26) and Torocheshnikov and Ershova (27), who studied argon-oxygen-nitrogen mixtures.

The main disadvantage of this method is the disturbance caused by withdrawing samples. This effect is greatest at low pressures when the quantity of vapor withdrawn for analysis is a large fraction of the total vapor in the vessel.

5

Flow Method

In the flow method, gas is passed slowly, at constant temperature and pressure, through an apparatus that is constructed so as to ensure good thermal and physical contact of the vapor phase with the condensed phase. The vapor phase is removed continuously and analyzed. The condensed phase is either removed continuously or is allowed to collect in a vessel for subsequent analysis.

Steckel and Zinn (28) used this method for studying mixtures of hydrogen, nitrogen, and methane; Ruhemann and Zinn (29) for studying hydrogen-nitrogen-carbon monoxide mixtures; Ruhemann (30) for studying methane-ethane mixtures; Guter, Newitt, and Ruhemann (31) for studying methane-ethylene mixtures; and Brown and Stutzman (32) for studying natural gas mixtures.

The principal advantage claimed for this flow method is that the vapor and condensed phases can conveniently be removed for analysis without upsetting equilibrium. The main disadvantage is that it is not certain that true equilibrium is achieved during this once-through process. Another serious disadvantage is the large quantity of test mixture required.

Circulation Method

In the circulation method, the vapor is withdrawn from the equilibrium vessel and continuously recirculated through the condensed phase. The phases are analyzed continuously, or at intervals, until a constant analysis is obtained. This ensures that equilibrium conditions have been reached.

Dodge and Dunbar (33) perfected this method while investigating the oxygen-nitrogen system. Rosanoff, Lamb, and Breithut (34) originated the method for use in binary mixture studies. It has been used by Torocheshnikov (35) for mixtures of carbon monoxide and nitrogen and by Torocheshnikov and Levius (36) for mixtures of nitrogen and methane. More recently, Benham and Katz (37) used the circulation method for studying hydrogen and light hydrocarbon systems; Maimoni (38) for studying hydrogen-nitrogen and duterium-nitrogen systems; and Cines, Roach, Hogan, and Roland (39) for studying methane-nitrogen systems.

6

SELECTION OF METHOD

Of the four methods of experimental investigation of phase behavior, all except the dew and bubble point method suffer from the common disadvantage that samples of the equilibrium phases must be taken without upsetting equilibrium. In addition these samples must be analyzed to determine the composition.

The flow method can be eliminated because it offers no apparent advantage in simplicity or accuracy over the circulation method and because the attainment of equilibrium is questionable. Also, inconveniently large quantities of test samples are required.

The batch method is very simple in design. However, even when special sampling techniques are used there is no positive assurance that the process of sampling does not disrupt equilibrium.

The circulation method has been acclaimed as the most accurate and reliable of the existing methods by Ruhemann (1). This method requires elaborate and complex equipment, and usually more time is required for calibration than has been allowed for this entire study.

The dew and bubble point method has the following advantages and was selected on the basis of these advantages. First, samples need not be taken and analyzed; thus, the requirement for elaborate analytical equipment is eliminated and the equilibrium is not disturbed by sampling. Second, the equipment is relatively simple. Third, it is especially well suited for investigations of three-phase phenomena. Fourth, the PVT data necessary for the preparation of thermodynamic charts can be obtained in the normal course of determining the phase boundaries. Fifth, the accuracy of this method is comparable to that of the circulation method, as indicated by a comparison of the data of Bloomer and Parent (7) with that of Cines, Roach, Hogan, and Roland (39).

SECTION 4

EXPERIMENTAL METHOD

BASIC METHOD

The basic principle of the experimental method used in this study is that
of the dew and bubble point method. This principle is very simple, and is
illustrated in Figure 4-1 for the case of a vapor-liquid determination. A
gas mixture of known composition is charged into a cell, of fixed volume,
at low pressure. The conditions after each successive addition of gas are
represented by the dots along line (1)-(2)-(3).

When the pressure at point (2) is reached, the liquid phase appears as
small droplets. One point on the dew point curve is thus established. Further
additions of gas result in the condensation of the gas until the cell is
completely full of liquid at (3). This point represents a point on the
bubble point curve. By repeating this process at different temperatures and
varying the gas composition, the vapor-liquid phase boundaries are established.

The dots along line (1)-(2)-(3) represents points at which PVT data can
be taken. This is done by careful measurement of the amount of gas added to
the cell with each addition. The temperature and pressure are measured and
the cell volume is known. Therefore, the PVT data necessary to evaluate the
thermodynamic properties of the mixture can be measured in the normal course
of determining the liquid-vapor phase boundaries. This is one of the major
advantages of this method over the other methods discussed in Section 3.

MODIFIED METHOD

The importance of the triple-point depression, or the determination of
solid-liquid-vapor equilibria behavior, is discussed in Section 7. By chang-
ing the experimental procedure described above, solid-liquid-vapor equilibria
data can be taken with the same apparatus. This method is similar to the one
used by Donnelly and Katz (40) and later used by Kurata and Kohn (9).

Starting at a temperature below T_1 in Figure 4-2, which represents a
complete phase diagram for a general gas mixture (9), gas at low pressure
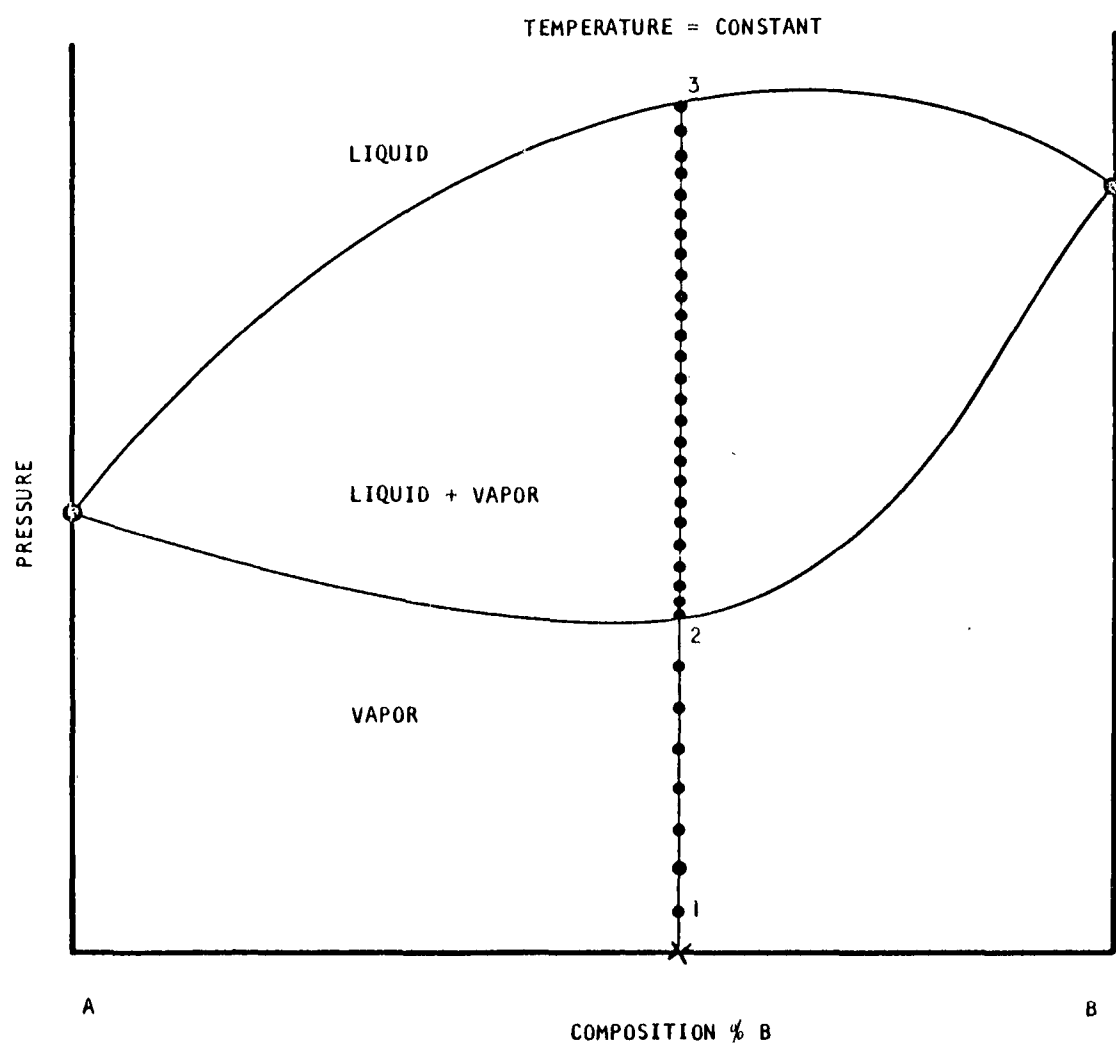
Figure 4-1.   General Dew and Bubble Point Diagram
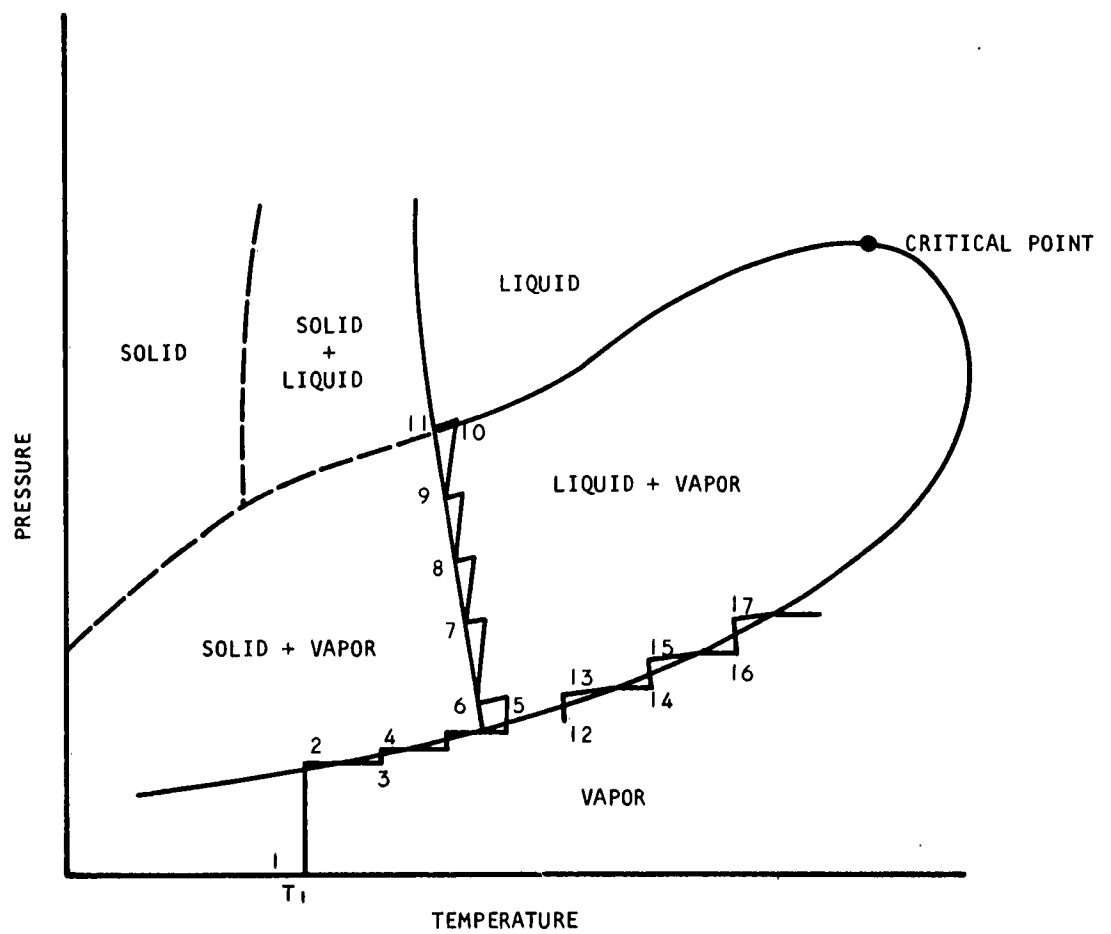
Figure 4-2. General Phase Diagram for a Gas Mixture

is charged into the equilibrium cell. The pressure is then increased by successive additions of gas. The process is indicated by line (1)-(2). At (2), the solid phase appears. The temperature is then raised a few degrees as indicated by line (2)-(3), and a point on the solid-vapor phase boundary is determined by noting the point where the solid disappears. Additional points are determined by increasing the pressure along line (3)-(4) and repeating the above process.

This procedure is repeated until the liquid phase appears in the cell, indicating that the liquid-vapor region has been reached. At this point sufficient gas is added to the cell to form a measurable liquid layer. This condition is represented by point (5). The cell is then slowly cooled until solid crystals are formed and the three phases coexist in equilibrium at point (6). Additional points on the three-phase line can be determined by alternately raising the cell pressure by addition of more gas and lowering the temperature as illustrated by points (7), (8), and (9).

A pressure is reached at which the equilibrium cell is full of liquid at (10). This is the bubble point at the measured pressure. The temperature can then be lowered along line (10)-(11), keeping the cell just full of liquid, until a minute amount of solid is formed at (11). This point is usually referred to as a crystal or solidus point. The locus of crystal points can be obtained by the procedure given above. This is unnecessary for the purpose of this study, since solid-liquid equilibria are of little interest as a means of refrigeration in aerospace applications.

The dew point curve of the mixture is determined as indicated by the processes (12)-(13)-(14)-(15)-(16)-(17). Starting at point (12), the cell pressure is increased by injecting gas into the cell until a finite drop of liquid is visible at point (13). The cell temperature is then increased until the drop of liquid is completely vaporized at point (14). The point at which the last drop of liquid is vaporized is a point on the dew point curve. As discussed in Section 6, a graphical method was used to determine the exact point of transition from the liquid to the vapor phase.

11

SECTION 5

EQUIPMENT AND EXPERIMENTAL PROCEDURE

GENERAL

The experimental apparatus designed for this investigation is a modifi-
cation of the Kurata and Kohn (9) apparatus, with features of the Bloomer and
Parent (7) apparatus incorporated. Figure 5-1 is a schematic diagram of the
apparatus, and Figure 5-2 is a photograph of the actual apparatus. The appa-
ratus is based on the dew and bubble point method and provides for determina-
tion of vapor-liquid equilibria, vapor-liquid-solid equilibria, and PVT data.

PRINCIPLES OF OPERATION

Prior to starting an experimental run it is necessary to prepare a gas
sample of known composition. This is accomplished by mixing known quantities
of pure gases. Referring to Figure 5-1, (A_1) and (A_2) are calibrated cylinders
made of heavy wall glass tubing. These cylinders are used to measure the vol-
ume of the pure components prior to mixing, to store the gas mixture, and to
measure the amount of gas forced into the equilibrium cell (I).

Subsequent to its preparation the gas mixture is added to increments from
the calibrated cylinder (A_1) and (A_2) to the equilibrium (I). As an inter-
mediate step, the gas enters the bulb on U-tube assembly (F). In (F) the pres-
sure is adjusted to any desired level by closing either valve (7) or (17) and
varying the volume of the fixed amount of gas trapped in the tubing and bulb.
This is accomplished by adjusting the level of the mercury in the U-tube and
bulb assembly.

The pressure within the cell is increased by successive additions of gas
from (A_1) or (A_2) via the U-tube and bulb assembly, and the temperature con-
trolled by regulating the pressure over a jacket liquid which surrounds the
cell. In this manner the temperature and pressure processes required to de-
fine the phase boundaries as described in Section 4, are performed.

The equilibrium cell (I) is made of heavy-walled pyrex glass tubing, and
is jacketed with a liquid bath to control its temperature. The temperature
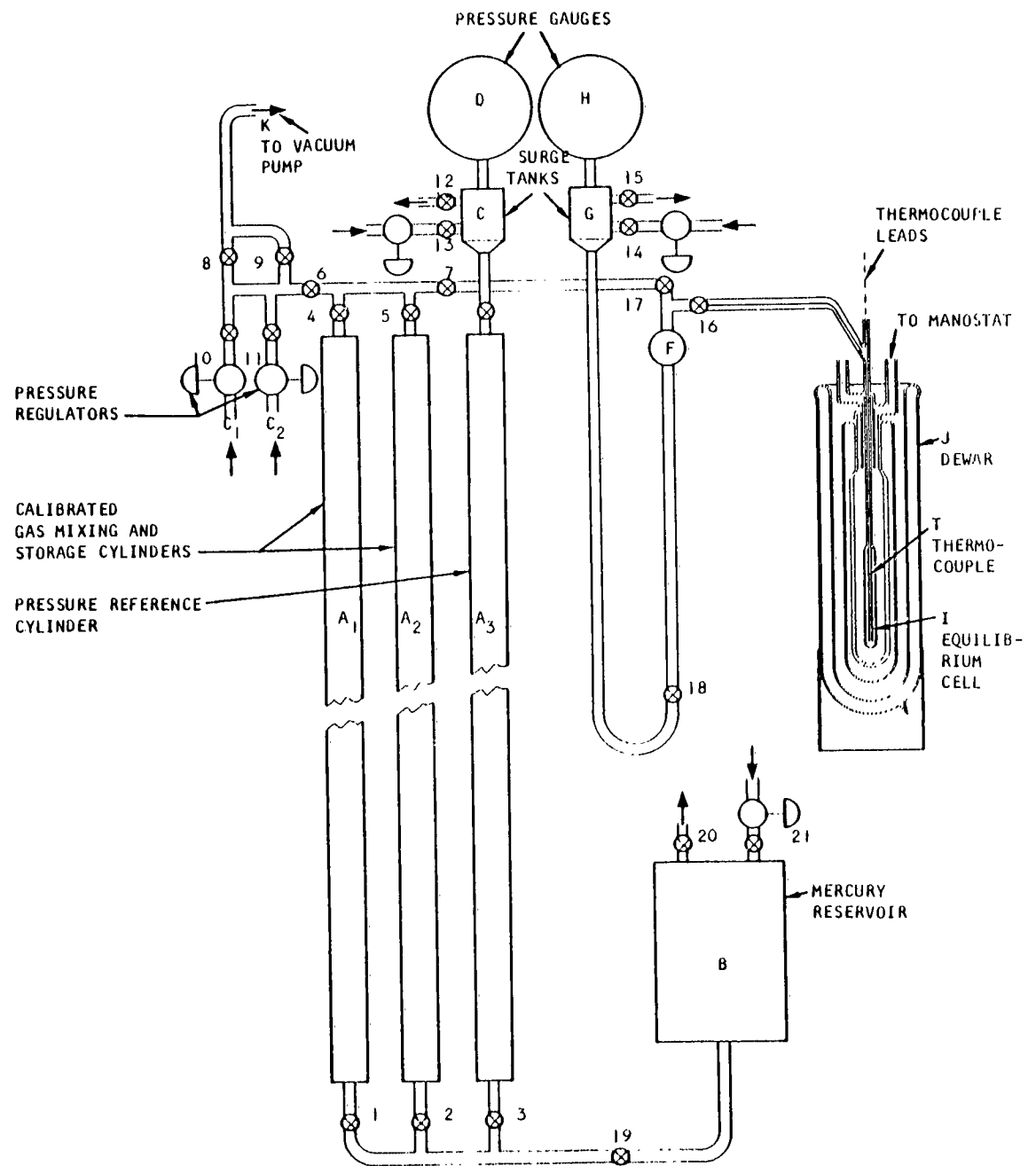
Figure 5-1. Apparatus Schematic Diagram
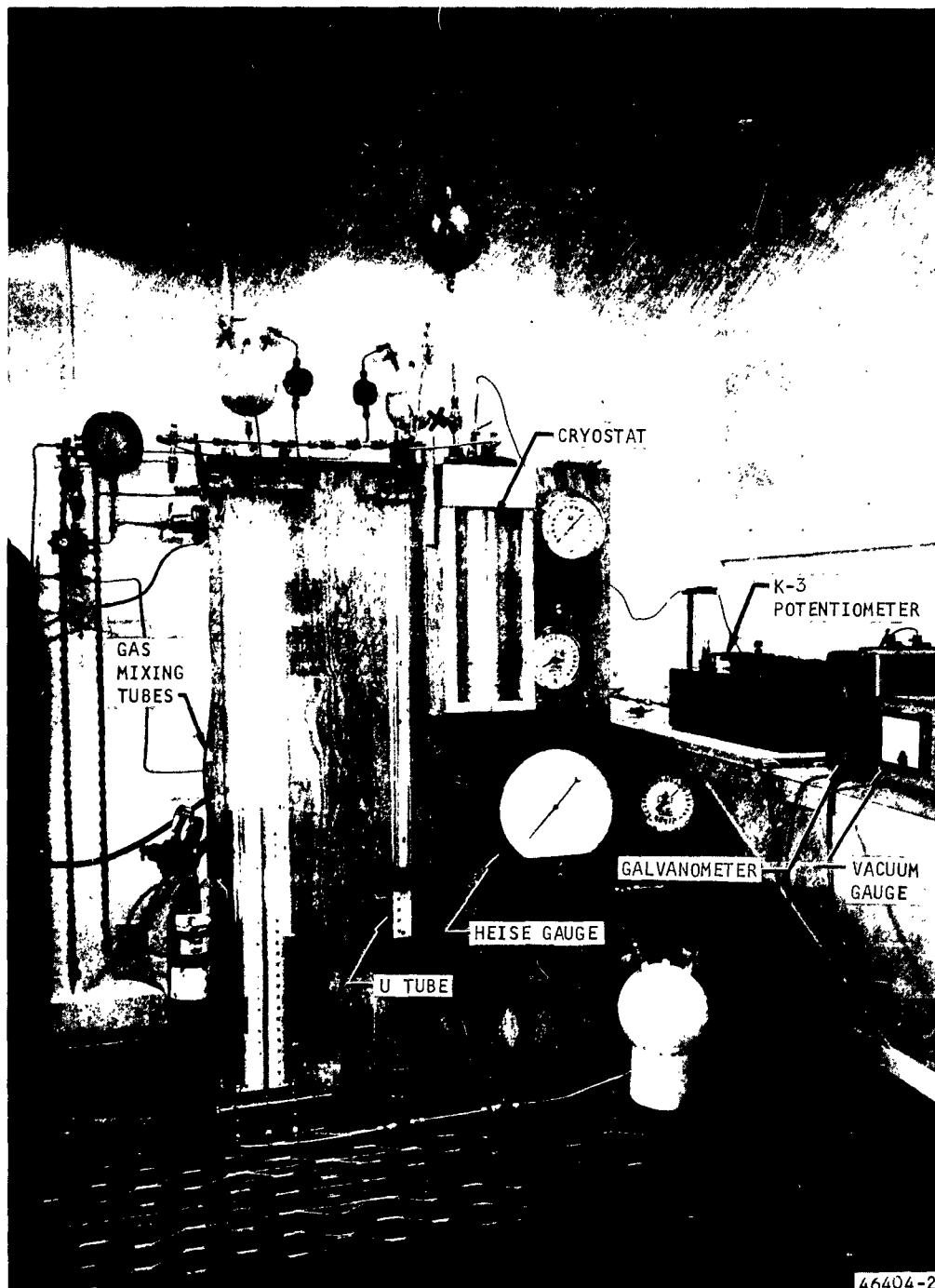
Figure 5-2. Overall View of Experimental Apparatus Used for
Binary Gas Mixture Property Determinations

is controlled by regulating the pressure over the jacket liquid. This means
of temperature control gives rise to certain limitations in the temperature
ranges that can be covered, as discussed subsequently. The temperature of
the cell is measured by thermocouple (T) and a high-precision potentiometer.
The thermocouple is located inside the cell; thus, the usual assumption of
the equality of cell and bath temperature is avoided. Positive cell pressure
is transmitted via the mercury U-tube and bulb assembly (F) and measured by
pressure gauge (H). Cell pressure below one atmosphere is measured by the
mercury U-tube directly.

BASIC CONSIDERATIONS

Before selecting this method, consideration was given to other methods
outlined in the literature. The circulation method looked particularly promis-
ing until some of its complexities were realized. The basic principle of the
dew and bubble point method was selected because it offered more versatility
with the same accuracy as more elaborate methods and entailed equipment of
greater simplicity.

Careful consideration has been given to the sources of error, so that
accurate data could be obtained. The equilibrium cell was made from glass
to allow visual observations of all phenomena. This is of particular impor-
tance in three-phase determinations. Pyrex glass was selected because of
its low coefficient of thermal expansion. This ensures a constant cell vol-
ume over wide temperature ranges. The cell is connected to the charging
apparatus by capillary tubing in order to maintain the ratio of cell volume
to total sample volume (downstream from valve (16)) as large as practical.
This permits uncertainties in volume measurements to be held to a minimum.

The capillary tubing extends into the equilibrium cell almost to the
bottom, as indicated in Figure 5-3. Thus, as an appreciable liquid level
is formed, a liquid seal is maintained between the cell and the external
capillary tubing. This inhibits diffusion in the line, brought about by
concentration gradients between the warm gas in the tubing and the contents
of the equilibrium cell. The conditions that would tend to alter the liquid
composition and upset equilibrium are thereby minimized.

VACUUM JACKET
DEWAR

OUTER JACKET
LIQUID

INNER VACUUM
JACKET

INNER JACKET
LIQUID

EQUILIBRIUM
CELL

THERMOCOUPLE

A-788
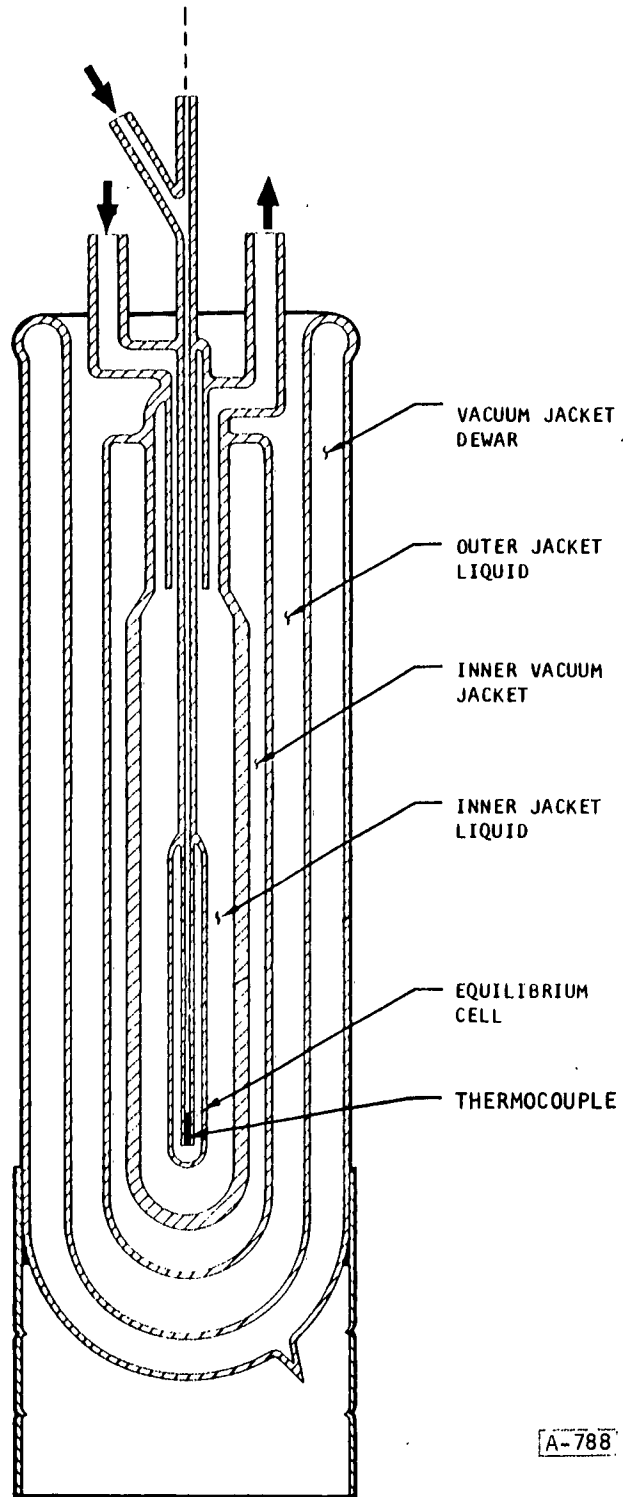
Figure 5-3.   Cryostat and Equilibrium Cell

DETAILS OF APPARATUS

Equilibrium Cell

The pyrex equilibrium cell is shown in some detail in Figure 5-3. Its internal volume is approximately 5 cu cm. The capillary tubing is extended to within 5 mm of the bottom of the cell to prevent diffusion, as discussed above. The cell is designed to withstand pressures in excess of 500 psia.

Gas Measurement and Storage

The volumetric measurements required for preparing the gas mixtures and measuring the amount of gas charged to the equilibrium cell are made in the glass cylinders (A_1) and (A_2). These cylinders have an internal volume of approximately 1000 cu cm each, and are shown in Figure 5-4. This provides sufficient gas at 200 psia in each cylinder to completely fill the 5 cu cm equilibrium cell with saturated liquid. Volumetric calibration curves were prepared for each cylinder by filling with mercury, making withdrawals, and weighing each volume withdrawn.

The cylinders are connected at the top by stainless steel tubing, as illustrated in Figure 5-4. The pressure within either cylinder is measured by reference to cylinder (A_3). By adjusting the height of the mercury in (A_3) to equal that of the active cylinder (A_1) or (A_2), the pressure of the active cylinder is read at pressure gauge (D). Pressure gauge (D) is a Bourdon-type gauge that is calibrated against a dead-weight gauge. The necessary adjustments are made with the pressure regulator (13) attached to the surge tank (C). The mercury is added to or withdrawn from cylinders (A_1), (A_2), and (A_3) as required by admitting or venting gas from the mercury reservoir (B).

Ports (C_1) and (C_2) of Figure 5-1 are connected to the storage bottles of the pure components. The component gases are charged to the mixing cylinders through pressure regulators (10) and (11), which reduce the pressure to any desired level under 200 psia.

Cryostat

The configuration of the cryostat is shown in Figure 5-3. The equilibrium cell is surrounded by a jacket of liquid. By controlling the pressure over this liquid, the temperature of the cell is regulated. The temperature of the liquid is uniquely defined by the pressure only so long as the pressure

CRYOSTAT

U TUBE

GAS
MIXING
TUBES

REFERENCE
TUBE

HEISE
GAUGE

46404-1
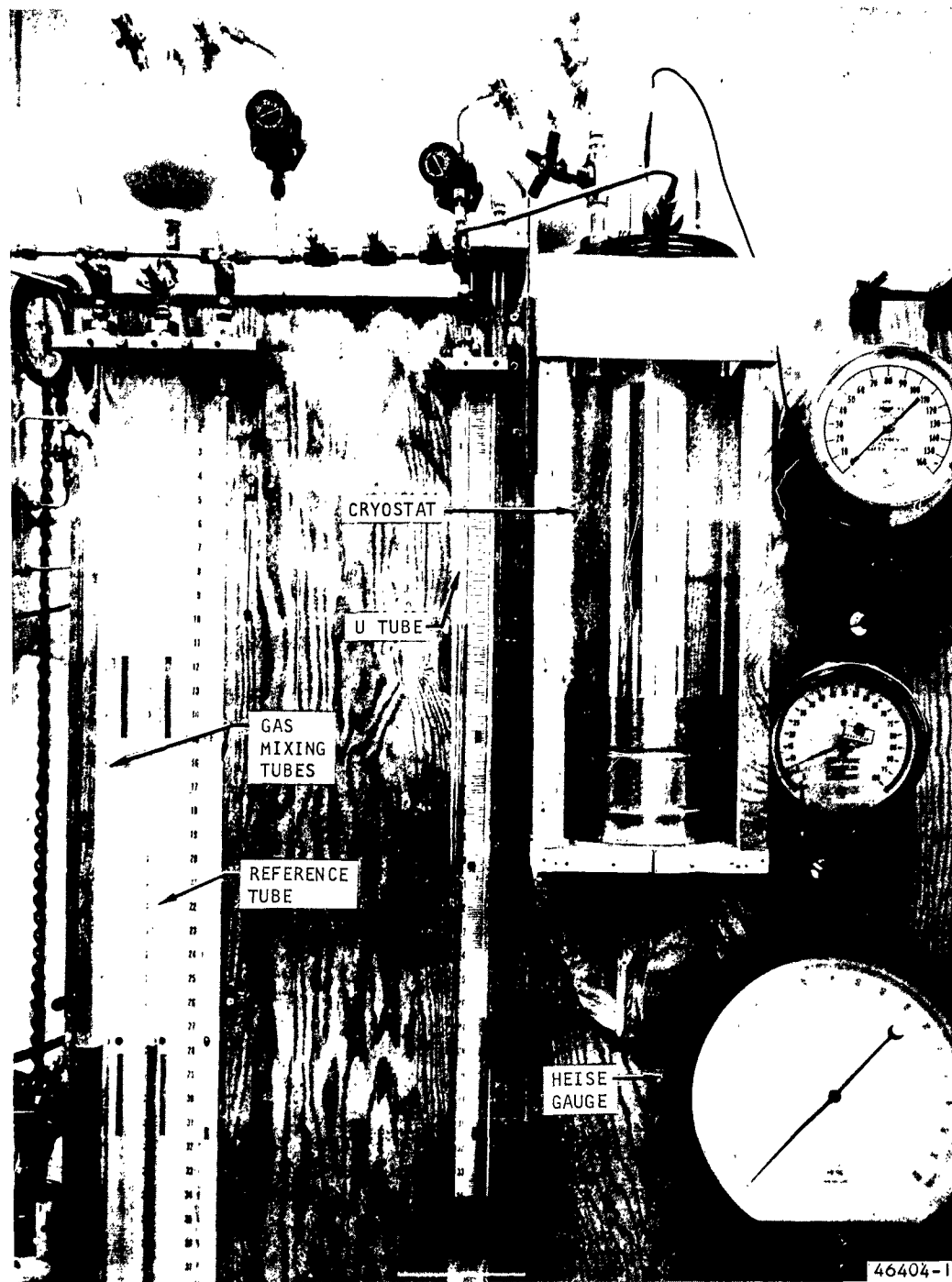
Figure 5-4. Closeup View of Panel Showing Gas Mixing Apparatus
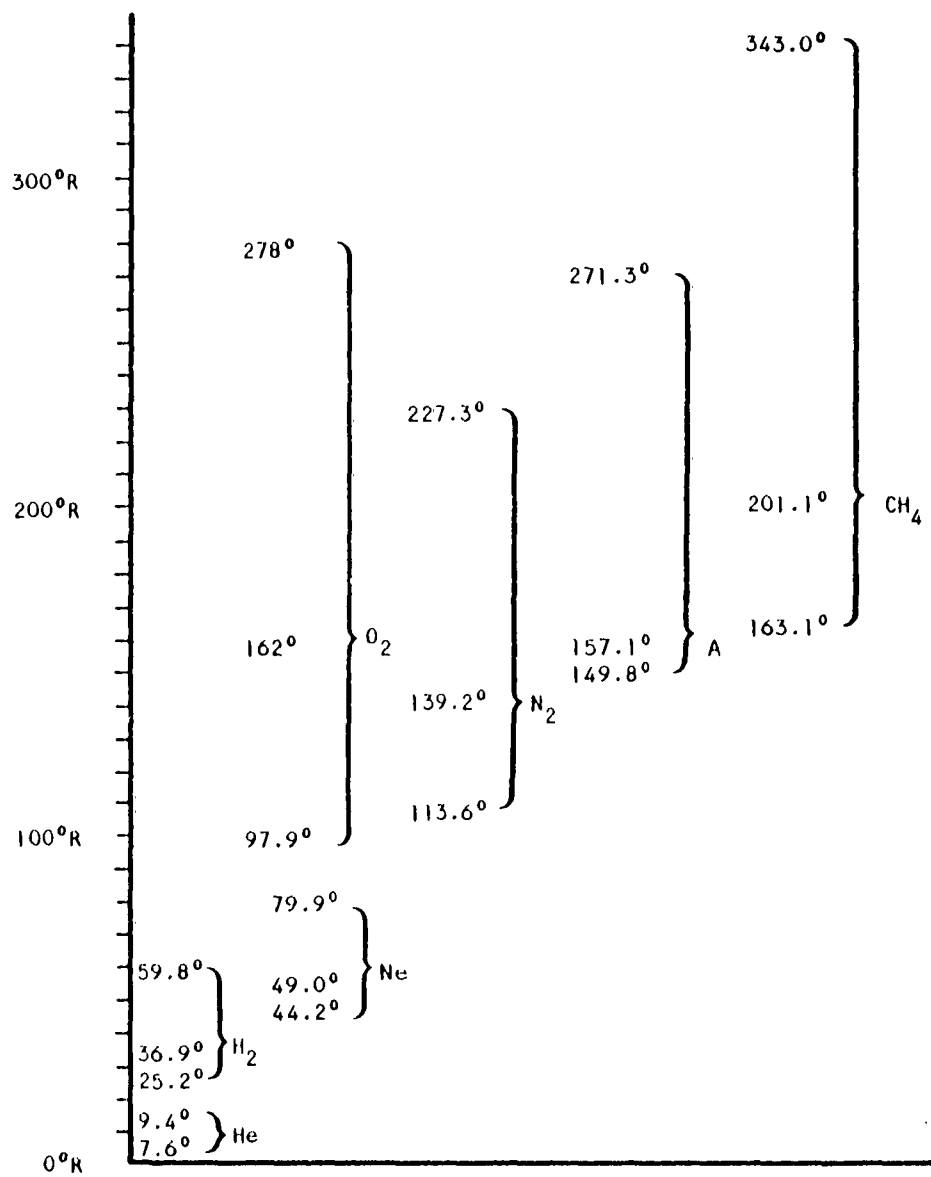
Figure 5-5.   Temperature Range Covered
by Two-Phase Cryostat

A-789

19

is below the critical point of the jacket liquid. Figure 5-5 gives the temperature ranges that can be covered with the various jacket liquids. This limitation can be removed by operating with the jacket fluids in the supercritical range and bleeding off fluid at a rate required to maintain isothermal conditions. However, because of the high pressure encountered and the additional controls required, this type of operation was not used in this study.

The internal jacket is shielded by a vacuum jacket to reduce the consumption of inner jacket liquid. This complete apparatus is immersed in a Dewar vessel filled with a second liquid to further reduce the heat leak and provide thermal stability. The components of the cryostat are shown in Figure 5-6, and the assembled cryostat is shown in Figure 5-7.

The thermocouple leads are placed in the capillary tube that connects the equilibrium cell to the gas charging apparatus. This arrangement reduces the dead volume in the sample space. An additional benefit is the tempering of the leads. The leads, in close proximity to the cell, are thus at the same temperature as the equilibrium cell. A thermal analysis of this arrangement shows that only 3/4 in. of lead is required to obtain a temperature reading within one percent of the cell temperature, for an outer jacket temperature of $140^{\circ}R$ and a cell temperature of $36^{\circ}R$.

Pressure Measurement

As previously mentioned, the U-tube and bulb assembly (F), shown in Figure 5-1, is used to adjust the pressure of the gas prior to charging it to the equilibrium cell.

This section of the apparatus also serves as the pressure gauge for the equilibrium cell. The cell pressure is transmitted by the mercury in (F) and measured by gauge (H). Gauge (H) is either a manometer or Heise gauge, depending on the pressure range.

Equilibrium Cell Temperature Measurement

The temperature of the cell was measured by a copper-constantan thermocouple connected to an L and N type K-3 potentiometer and an L and N type E self-contained galvanometer. Using this equipment, temperature changes on the order of $0.03^{\circ}K$ were detectable. The thermocouple was calibrated in place to ensure maximum accuracy.

OUTER DEWAR VESSEL

1/2 INCH WINDOW

VACUUM SHIELDED INNER ASSEMBLY
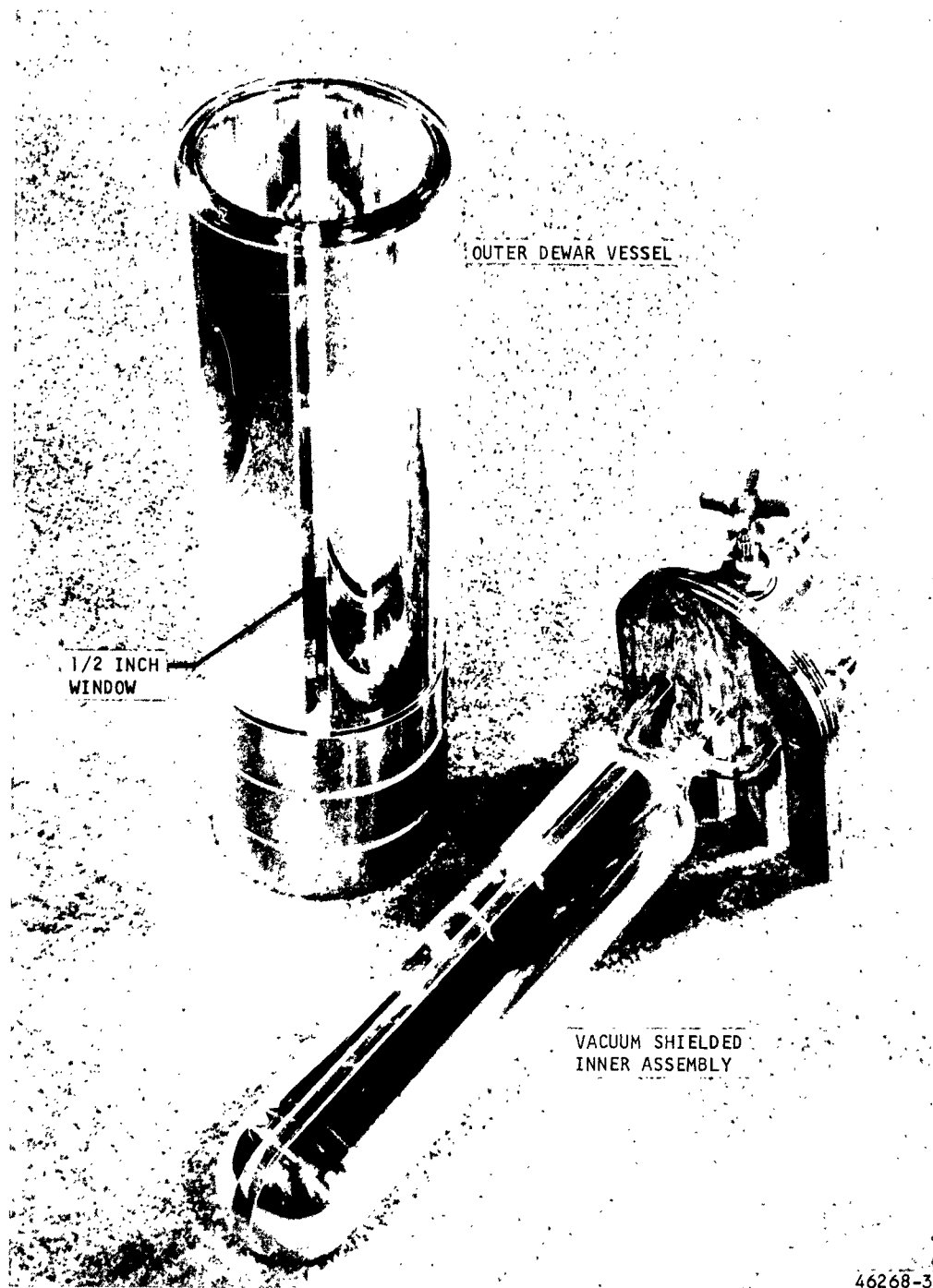
46268-3

Figure 5-6. Cryostat with Inner Dewar Assembly Removed

THERMOCOUPLE WELL

MANOSTAT
CONNECTION

EQUILIBRIUM
CELL CONNECTION
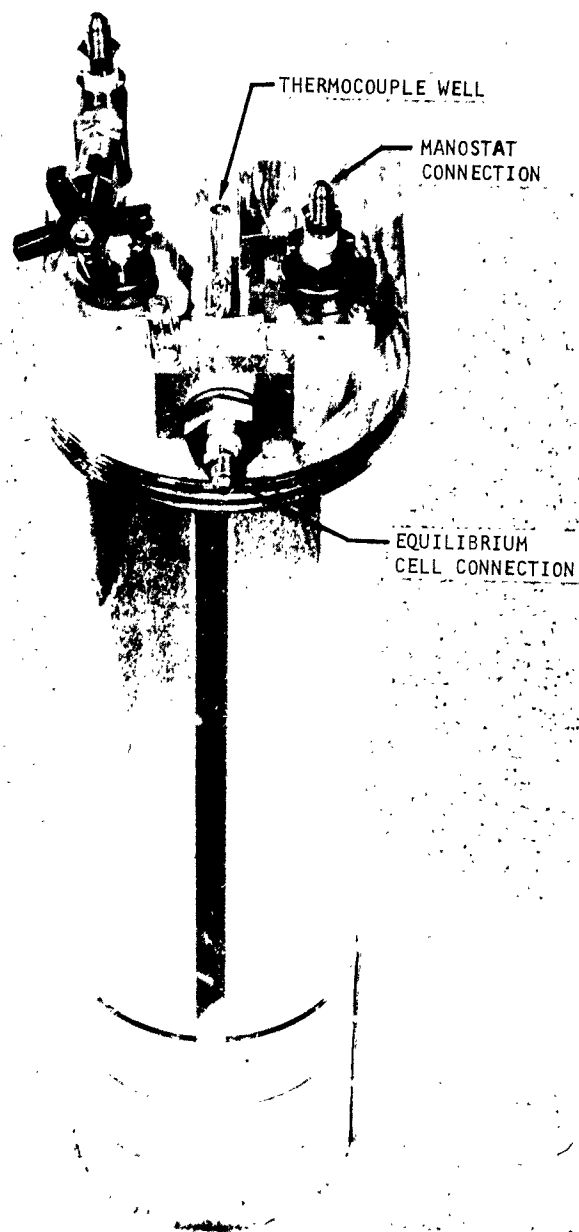
46268-1

Figure 5-7. Assembled Cryostat

EXPERIMENTAL PROCEDURE

Preparation of Mixtures

Referring to Figure 5-1, the initial step is to bleed a little of each component from (C_1) and (C_2). The apparatus is then evacuated by opening valves (4), (5), (6), (7), (8), (9), (16), and (17), closing all other valves, and drawing a vacuum at (K). The vacuum pump at (K) was capable of evacuating the system to 10^{-5} mm of Hg. It also was equipped with a vacuum gauge to indicate when the system was sufficiently evacuated.

After the apparatus is evacuated, valves (7), (8), (9), (16), (17), and either (4) or (5) are closed. The space above the mercury is either (A_1) or (A_2) and is charged from (C_1) or (C_2) as desired. The pressure regulators (10) and (11) reduce the pressure approximately 100 psia. By adjusting the height of mercury in (A_1) or (A_2), then varying the pressure in (B), and bleeding off small amounts of gas through needle valve (9), exact volumetric control is achieved. The charged cylinder is then closed off, and the connecting tubes are again evacuated. The second component is charged to the remaining cylinder in a like manner. The temperature of the mixing and storage cylinders is then taken and the pressure of each cylinder is measured by reference to (A_3), as described previously.

The tubing is evacuated a third time, and valve (6) is closed. The components are then mixed by opening valves (4) and (5), and forcing the gas back and forth by alternately raising the level of the mercury in (A_1) and (A_2). After repeated mixing, the binary mixture is ready for testing.

The exact amount of each gas contained and the composition of the mixture is then computed from published compressibility factors for the pure components and the above measurements.

Charging of the Equilibrium Cell

Much of the operating procedure has been presented in describing the component parts of the apparatus. At the risk of being repetitious, the operating procedure will be summarized here.

Upon completion of mixing as described above, gas mixture of known composition is contained in cylinders (A_1) and (A_2). Cylinders (A_1) and (A_2) are then used separately to charge gas into the equilibrium cell in the following manner. Gas mixture is charged into the section of tubing between valves (7) and (16) in Figure 5-1, with mercury level U-tube at a fixed point. The pressure in this section is made equal to the original pressure of the gas in the applicable storage cylinder by adjusting the level of the mercury in the storage cylinder and checking against pressure gauge (D) and cylinder (A_3). Valve (7) is then closed and the mercury level in the U-tube and bulb assembly (F) is adjusted until the desired volume of charge exists over the mercury. Valve (17) is then closed and the charge pressure adjusted by means of regulator (14) and/or valve (15). With valve (17) closed and (16) open, the gas is charged into the equilibrium cell by displacing the gas from the U-tube and bulb assembly (F) with mercury.

After sufficient time has elapsed to establish equilibrium, the cell temperature and pressure are recorded. Valve (16) is then closed and the tube between valves (7) and (16) is recharged at the same pressure as before. From the change in the level of the mercury in the active cylinder (A_1) or (A_2) the amount of gas charged to the cell in the previous step is computed.

By repeating this procedure, PVT data can be taken as the successive additions of mixture are charged into the cell. Once the first phase boundary has been reached, either the standard dew and bubble point procedure or the modified method of Kurata and Kohn can be followed. These two procedures were outlined in Section 4.

•

24

SECTION 6

EXPERIMENTAL DATA AND ITS EVALUATION

DATA PRESENTED

The experimental data presented in this section include the following:

a.   The solid vapor, dew point, bubble point, and three-phase boundaries for a 0.23 percent neon in argon mixture over the temperature range of 80.6°K to 100°K.

b.   The dew-point curves for four mixtures of neon and argon, ranging in composition from 0.23 to 49.97 percent neon. The temperature range covered extends from the point of intersection with the three-phase line up to 103°K.

c.   The solid vapor, dew point, bubble point, and three-phase boundaries for a 43.17 percent nitrogen mixture with argon between 67.4°K and 73.8°K.

ACCURACY EXPECTED

The accuracy of the various measurements is discussed briefly in Section 5. This discussion will be expanded here. The variables measured or calculated from measurements consist of temperature, pressure, and composition. The errors associated with each variable will be discussed in that order.

Temperature Mensuration Errors

The equilibrium cell temperature was measured with a copper-constantan thermocouple utilizing a Leeds and Northrup Type K-3 Potentiometer and Type E Guarded Galvanometer as readout equipment. The resolution of this equipment over the temperature range covered is ± 0.03°K. The absolute accuracy is dependent on the accuracy of the calibration. The thermocouple was calibrated at three points: the triple point of nitrogen (63.16°K), the boiling point of nitrogen (77.40°K), and the triple point of argon. The triple point of argon was taken as 83.85°K [41]. It was later discovered that 83.77°to 83.78°K might be a better value (see Reference 42). In view of this discrepancy, the accuracy will be taken as ± 0.1°K.

Pressure Mensuration Errors

Pressures below one atmosphere were measured with a mercury manometer that could be read to within ±0.1 in. Hg or approximately ±0.025 psi. Pressures above one atmosphere were measured with a 100 psig range Heise Gauge. This gauge was previously calibrated and has a maximum error of ±0.1 psi. To be conservative and account for small fluctuations in atmospheric pressure between barometric pressure checks, the pressure measurements will be considered accurate within ±0.1 psi.

Composition Errors

Errors in composition can arise from three sources: the purity of gases prior to mixing; errors in pressure, temperature, and volume data used to calculate the composition; and the degree of mixing achieved.

After completion of the mixing procedure given in Section 5, the mixture was allowed to stand for a 24-hour period prior to use. It was assumed that any possible concentration gradients were eliminated by diffusion during this period and the degree of mixing was taken as 100 percent.

The high purity gases used were obtained from the Linde Company and are stated to have the following purity:

TABLE 6-1

IMPURITIES IN PARTS PER MILLION BY VOLUME

Impurity	Neon	Argon	Nitrogen
Nitrogen	50	10	*
Helium	100	0	
Hydrogen	5	1	
Oxygen	5	5	
Hydrocarbons	15	5	
Moisture	3	3	
Total	178	24	24
Percent Purity	99.9822	99.9976	99.997

* Exact nature of impurities was not furnished for nitrogen.

To check the purity of the argon and nitrogen, the difference between the dew and bubble point pressures was determined over a moderate range of temperatures. In no case did the difference exceed 0.1 psi, which is within the range of experimental accuracy. It was, therefore, concluded that for all practical purposes these gases could be considered pure. To run the same check on the purity of the neon would require the use of liquid hydrogen as a coolant. Because of the special preparation required to provide adequate safety when using liquid hydrogen, this test was not performed and the purity stated above was assumed to be correct.

The fractional error per mole fraction can be expressed as the following function of the pressure and volume measurements:

$$\frac{\Delta X_1}{X_1} = \frac{(P_2 V_1 V_2 Z_1 Z_2)\ \Delta P_1\ +\ (P_1 V_1 V_2 Z_1 Z_2)\ \Delta P_2}{(P_1 V_1 Z_2 + P_2 V_2 Z_1)\ (P_1 V_1 Z_2)}$$

$$+\ \frac{(P_1 P_2 V_2 Z_1 Z_2)\ \Delta V_1\ +\ (P_1 P_2 V_1 Z_1 Z_2)\ \Delta V_2}{(P_1 V_1 Z_2\ +\ P_2 V_2 Z_1)\ (P_1 V_1 Z_2)}$$

$$+\ \frac{(P_1 P_2 V_1 V_2 Z_2)\ \Delta Z_1\ +\ (P_1 P_2 V_1 V_2 Z_1)\ \Delta Z_2}{(P_1 V_1 Z_2 + P_2 V_2 Z_1)\ (P_1 V_1 Z_2)} \qquad (6\text{-}1)$$

where

$\dfrac{\Delta X_1}{X_1}$ = Fractional error in the mole fraction of component 1

P_1 and P_2 = Pressure of components 1 and 2, respectively

ΔP_1 and ΔP_2 = Errors in the above pressure measurements

V_1 and V_2 = Volume of components 1 and 2, respectively

ΔV_1 and ΔV_2 = Errors in the above volumetric measurements

Z_1 and Z_2 = The compressibility factors of components 1 and 2, respectively

ΔZ_1 and ΔZ_2 = Deviations in the above compressibility factors

The above equation was derived on the assumption that the volumetric and pressure measurements were made at the same temperature. This should be a fair assumption, since the tests were run in an air-conditioned laboratory and the gases were injected into the mixing tubes and allowed to stand for a minimum period of one hour prior to measurement. At first sight the error given by Equation 6-1 appears to be independent of temperature. However,

since Z_1 and Z_2 are functions of temperature and pressure, the ΔZ's are functions of the accuracy with which the variables are measured, and the fractional error is an implicit function of the temperature and pressure measurements. The accuracy of the various mole percents, as determined by Equation 6-1, is given with the experimental data.

The volumetric measurements and the values of ΔV_1 and ΔV_2 in Equation 6-1 are functions of the geometry of the gas mixing tubes and the accuracy of determining the height of mercury in these tubes. The inner cross-sectional area of the gas mixing tubes is 1.23 sq in. By using a reference line on both sides of the mixing tubes, it was possible to eliminate errors due to parallax, and the height of the mercury could be determined within 0.02 in., which corresponds to a ΔV term of 0.0246 cu in.

In the case of mixtures of low concentration, the error due to the volumetric measurement is of particular importance and the reference line to eliminate the parallax was a necessity. In cases where an appreciable amount of both components was mixed, the reference line was not used; and it is estimated that the ΔV terms were 0.05 cu. in. in these cases.

EXPERIMENTAL DATA

The second method, or the method presented by Kurata and Kohn [7] as discussed in Section 4, was used to obtain the experimental data presented in this report.

Mixtures of Neon and Argon

1. Phase Boundaries at Low Neon Concentration

Figures 6-1 through 6-4 present the data obtained on a 0.23 ±0.06 percent neon in argon mixture. In Figures 6-1 through 6-3, the logarithm of the pressure is plotted versus the reciprocal of the absolute temperature. The straight lines resulting from these plots are convenient for extrapolating the data over a somewhat greater range if desired.

The data points plotted in Figure 6-1 represent the case in which a finite, but very small, amount of solid was visible within the equilibrium cell. The transition of a trace of solid into the vapor phase (i.e., the disappearance of the solid phase from the equilibrium cell as the temperature

28
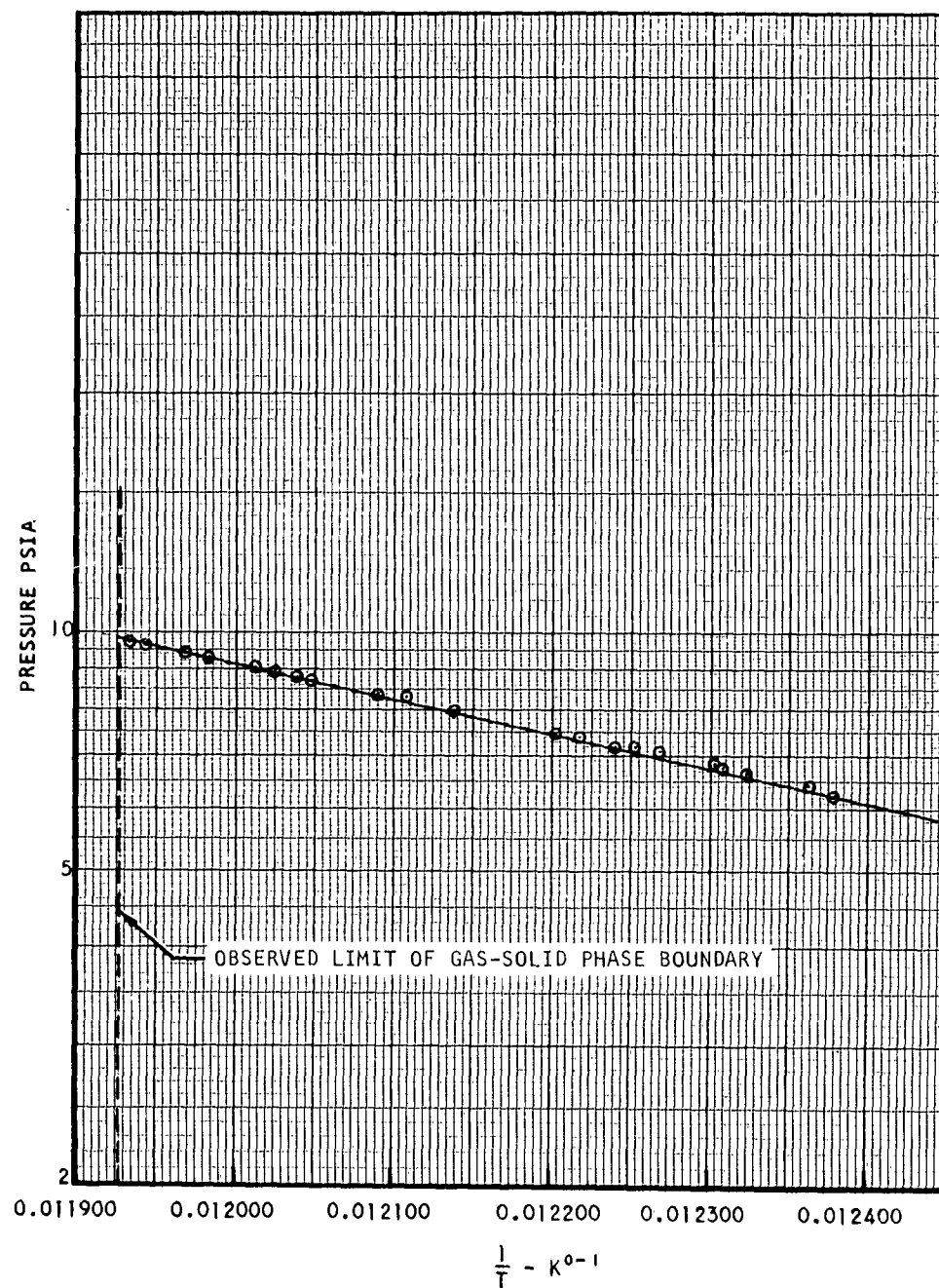
Figure 6-1. Gas-Solid Phase Boundary of
0.23 Percent Neon In Argon

A-790

was increased) was particularly easy to observe. This permitted plotting the gas-solid phase boundary with a minimum number of data points.

Visual determinations of the exact point of transition from the last drop of liquid in the equilibrium cell into the gas phase proved more difficult than in the case of solid-vapor transitions. The circled data points in Figure 6-2 represent points where liquid was no longer visible within the equilibrium cell. The points enclosed by squares represent points where a small, but finite, drop of liquid was visible.

Two important factors are indicated by the presence of a number of circled points on the line drawn through the point representing a two-phase system. First, it is evident that visual determinations of the point where the last drop of liquid disappears are not reliable. Apparently a trace of liquid remains in the cell, wetting the surface area around the thermocouple, which cannot be detected visually. Second, condensation of a small drop of liquid from the saturated vapor apparently does not greatly affect the composition of the vapor phase. This is reasonable since the liquid phase or drop is undoubtedly rich in argon, and condensing a small amount of argon-rich liquid from a gas mixture that is 99.77 percent argon would not change the concentration of the vapor phase significantly. In later experimental runs, where the neon concentration was higher, the converse was true, and graphical methods were employed to determine the transition or true dew points.

Figure 6-3 presents the data taken along the bubble point curve. The data points represent conditions where a faintly discernible bubble of vapor existed within the equilibrium cell.

Figure 6-4 presents the phase diagram obtained by combining the data plotted in Figures 6-1 through 6-3. In addition, three points on the three-phase line were determined and plotted. These points illustrate that no measurable triple-point depression was obtained. The large difference between the dew and bubble point pressures at a given temperature indicates that neon is only slightly soluble in the liquid phase at moderate pressures. Therefore, it would be anticipated that large triple or three-phase point depressions would not occur in mixtures of higher neon concentrations at moderate pressures. The subsequent runs at higher neon concentrations proved this deduction to be correct.
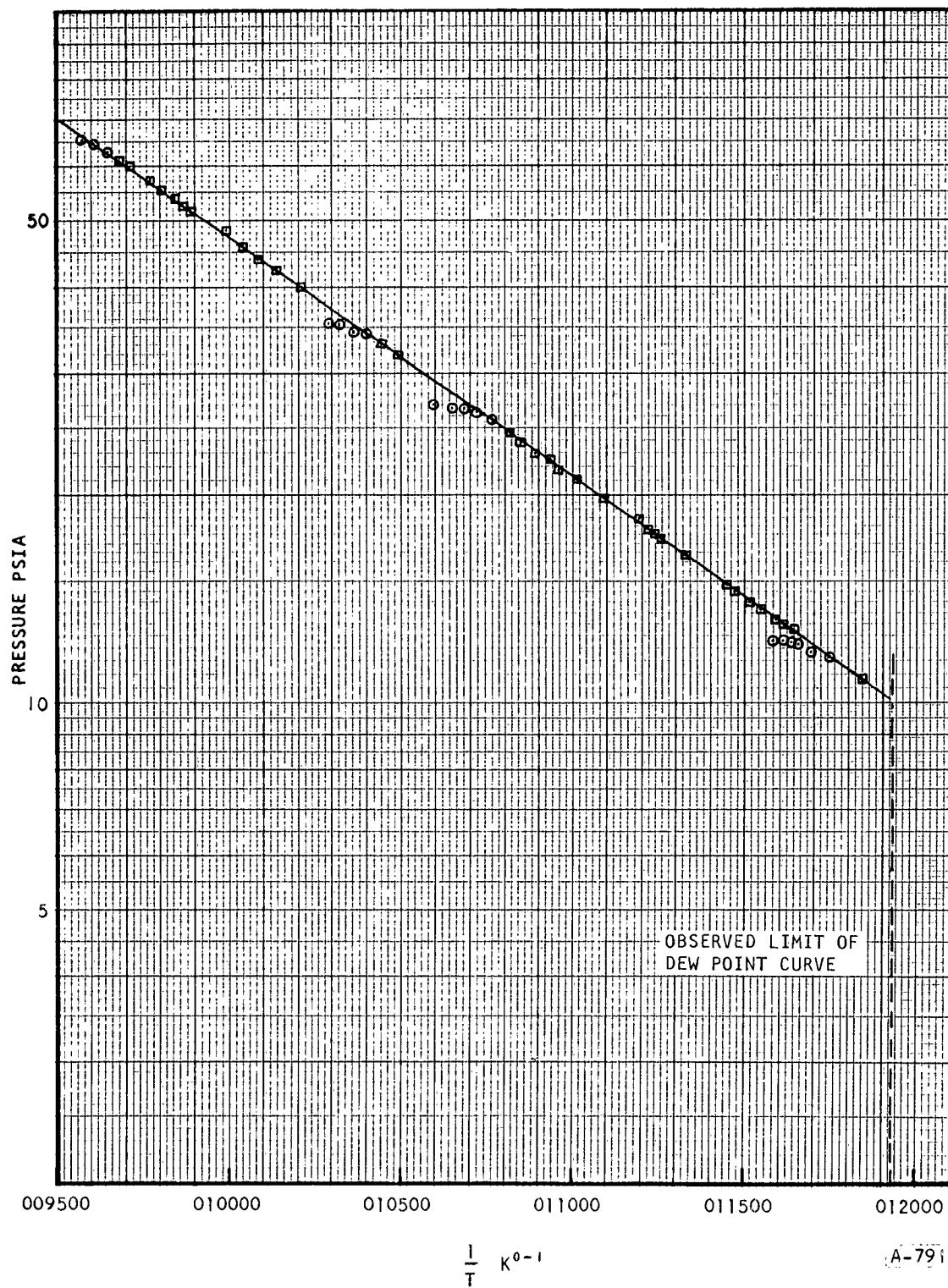
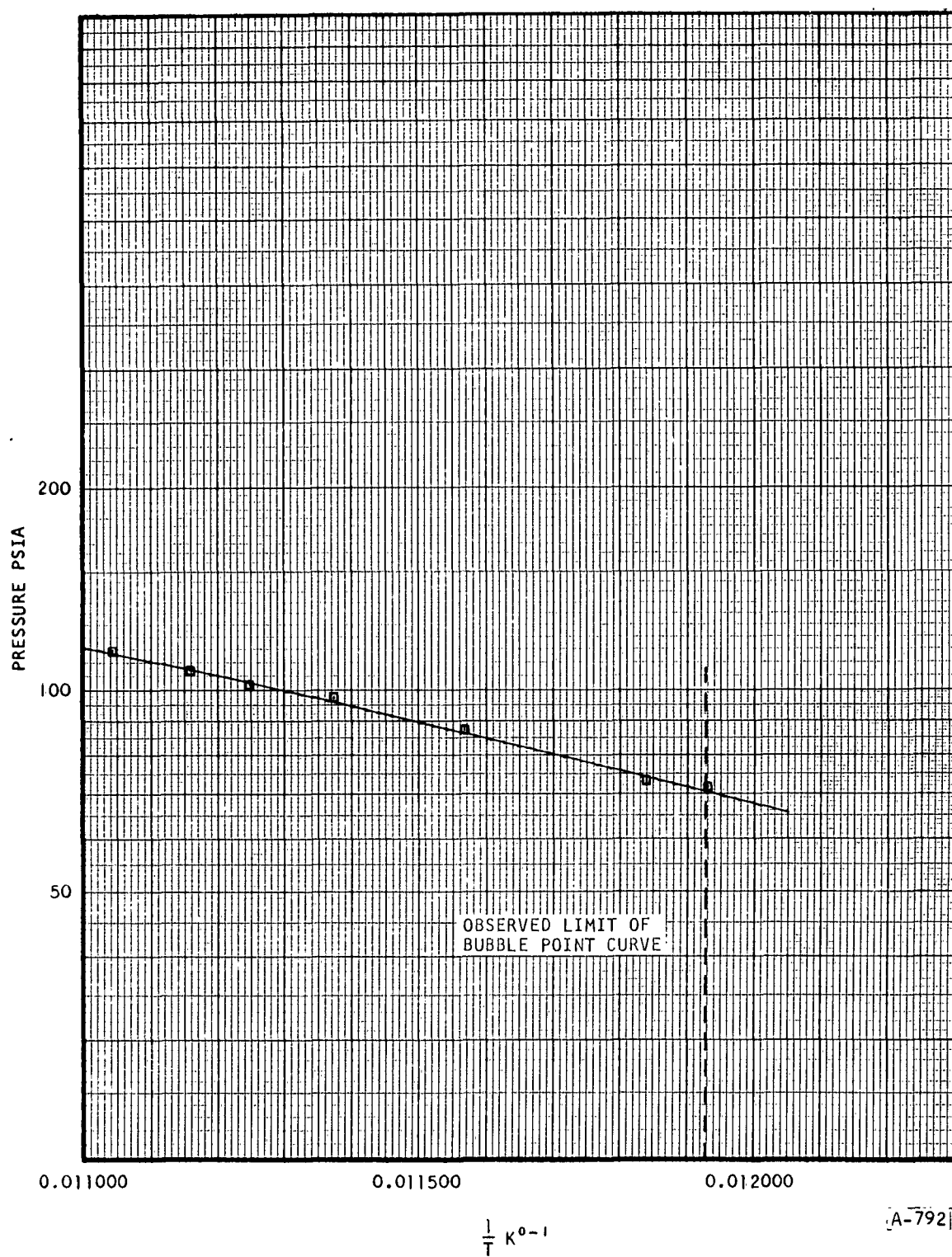Figure 6-2. Dew Point Curve of
0.23 Percent Neon in Argon

51
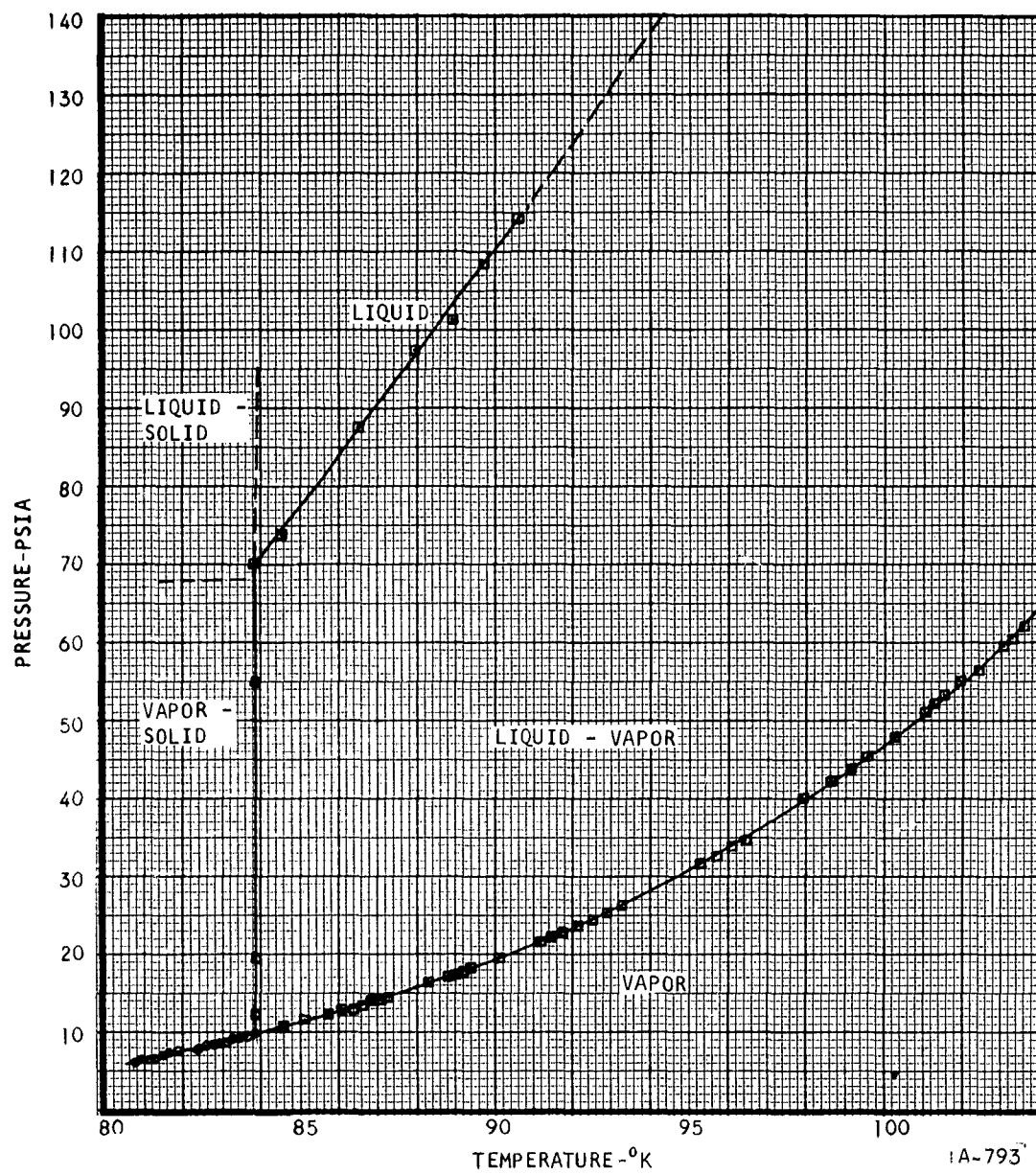
Figure 6-3. Bubble Point Curve of
0.23 Percent Neon In Argon

32

Figure 6-4. Phase Boundaries for 0.23 Percent Neon in Argon

2. Dew Point Plots

Figure 6-5 presents the dew point curves of four different mixtures of neon and argon. The curves are numbered 1 through 4 in order of increasing neon concentration. The points where the dew point curves cut the dashed line represent the intersection of the dew point curves with the solid-vapor and three-phase boundaries.

Curve 1 represents the same data as that presented in Figure 6-2. A graphical technique was employed to plot Curves 2 to 4. As previously mentioned, it was difficult to visually determine the exact point where the last drop of liquid in the equilibrium cell was completely evaporated. By making a series of cell pressure versus temperature measurements through each boundary transition, a series of plots, as illustrated by the examples in Figure 6-6, was obtained. In this figure, the lines with slight curvatures and greater slopes represent the case where a trace of liquid was visible within the cell. The straight lines represent conditions in the gas phase. The intersection of the two lines was taken as a dew point of the mixture under investigation. Points obtained in this manner were plotted to construct the smooth curves in Figure 6-5.

The vapor pressure or dew point curve of pure argon is given by Equation 6-2[42]:

$$\log_{10} P = 6.9224 - \frac{352.8}{T} \qquad (6\text{-}2)$$

where $T =$ the temperature ^{0}K (83.77 to 88.2 ^{0}K)

P = the pressure in mm of mercury

Curve 1, Figure 6-5, agrees with Equation 6-2 to within 0.2 psi at temperatures near the triple point of argon and to within the experimental accuracy of 0.1 psi at slightly higher temperatures. This close agreement is expected in view of the low neon concentration and its apparent slight solubility in the liquid argon phase. Thus, for practical purposes, Curve 1 can be considered as pure argon. Curves 2, 3, and 4 then represent the effect of increasing the concentration of neon.

Figure 6-5 indicates that no measurable change in the temperature at the intersection of the dew point curve with the vapor-solid and three-phase

34
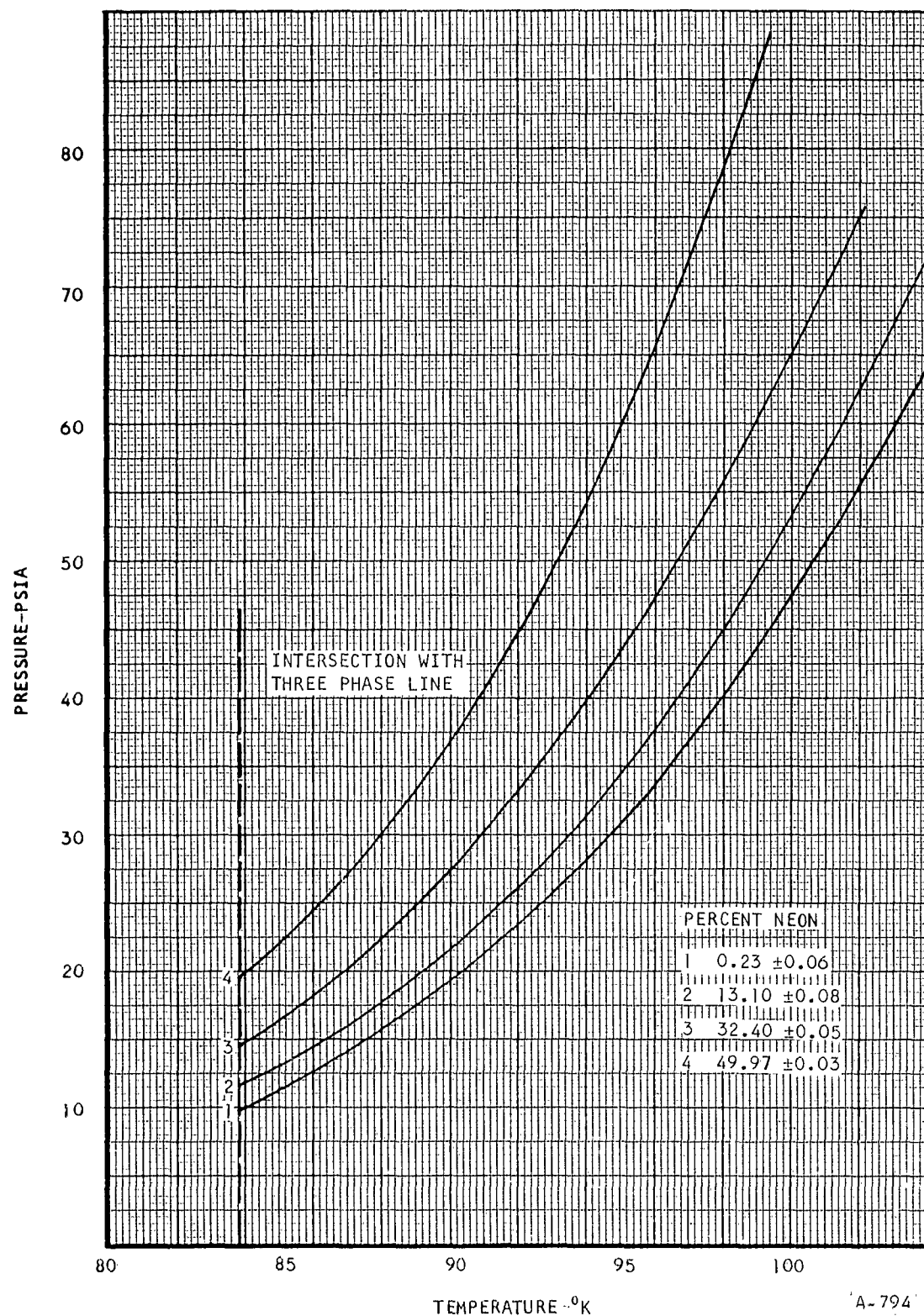
Figure 6-5. Dew Point Plots of Neon-Argon Mixtures

35
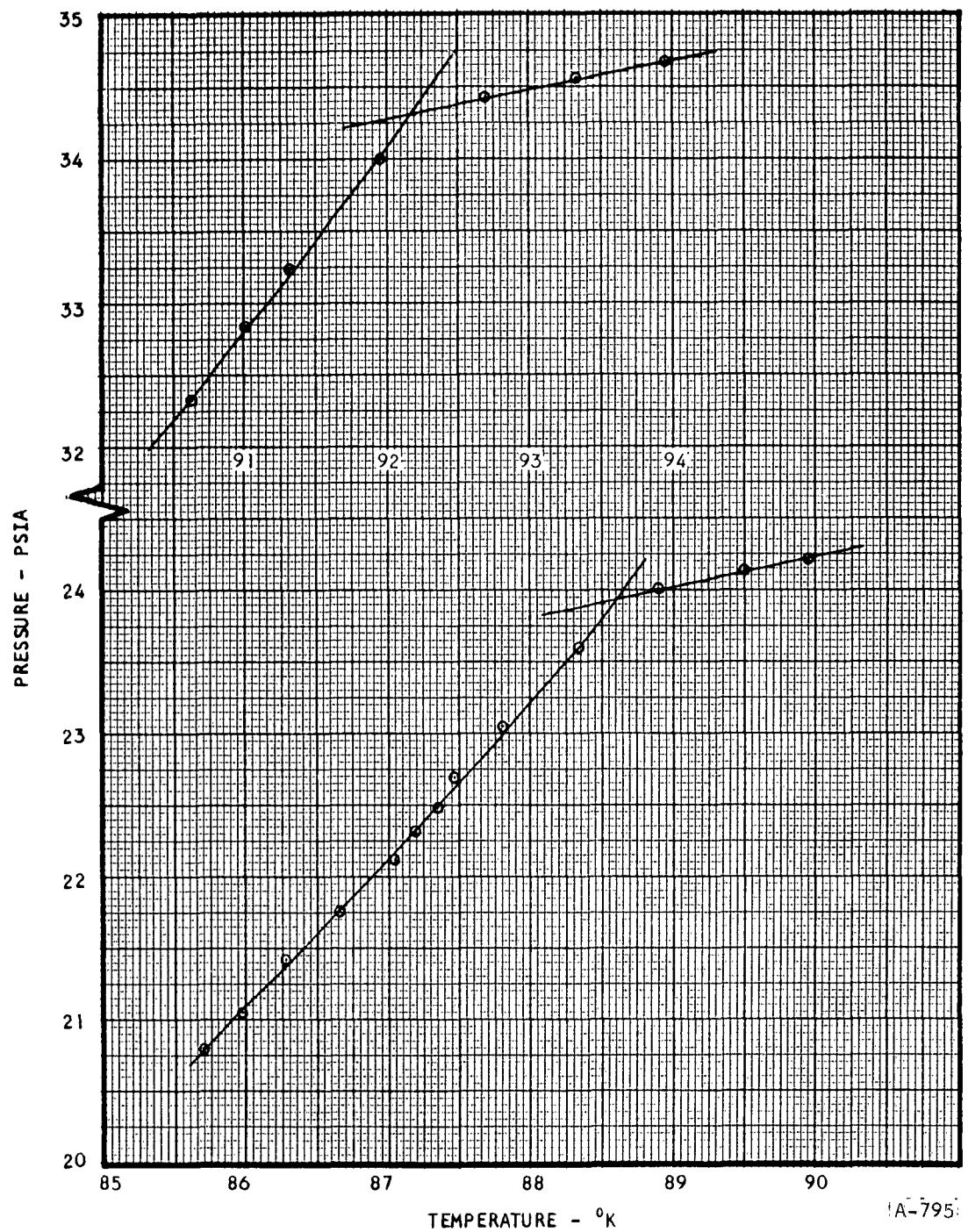
Figure 6-6. Graphical Points for Curve 3, Figure 6-5

36

boundaries occurred as the neon concentration was increased. To
investigate the validity of the observation, the following simplified
analysis was conducted.

When two or more phases coexist in equilibrium, it is a well-known fact
that the fugacity of a given component must be equal in all phases. If the
liquid and vapor phases are considered, the above thermodynamic law is
expressed by

$$fi_\ell = fi_v \qquad (6\text{-}3)$$

where fi_ℓ and fi_v = the fugacity of the ith component in the
liquid and vapor phases, respectively

Considering the argon in the system under investigation, Equation 6-3 can
be written as

$$\gamma X\, f_\ell = \phi y\, f_v \qquad (6\text{-}4)$$

where f_ℓ and f_v = the fugacity of the pure liquid and vapor, respec-
tively, at the same temperature and pressure

x and y = the mole fraction of the argon in the liquid and
vapor phases, respectively

γ and ϕ = the fugacity coefficient in the liquid and vapor
phases, respectively

If it is now assumed that the liquid phase obeys Raoult's Law and both phases
are ideal, Equation 6-4 becomes

$$x\, P_\ell = y\, P_T \qquad (6\text{-}5)$$

where P_ℓ = the vapor pressure of the pure argon at the same temperature

P_T = the total pressure

If the amount of neon in the liquid phase is neglected (i.e., $x \approx 1$),
Equation 6-5 reduces to

$$\frac{P_\ell}{y} = P_T \qquad (6\text{-}6)$$

Figure 6-7 presents a plot of Equation 6-6 compared with the data in Figure 6-5. The solid curves represent the data and the dashed lines represent Equation 6-6 at the same composition in the vapor phase. Because of the low pressures involved, the gas phase can be considered ideal, and the deviations of the curves in Figure 6-7 can be attributed entirely to the solubility of the neon in the liquid phase.

The close approach of the curves in Figure 6-7 indicates that neon is only slightly soluable in the liquid phase. Thus, with the vast predominance of argon in the liquid phase, it would be most unusual if the liquid phase did not follow Raoult's Law. Therefore, Equation 6-5 should be a good approximation and allow the liquid phase composition to be calculated with some degree of confidence. The liquid phase composition can then be used to calculate the three-phase or triple-point depression in the following manner.

Equation 6-7[43] expresses the triple point of a solution as a function of the composition of the liquid phase:

$$\text{Ln } X_\ell = \frac{\overline{\Delta H}_f}{R} \left(\frac{1}{T_o} - \frac{1}{T}\right) \tag{6-7}$$

where $\overline{\Delta H}_f$ - heat of fusion of the argon

T_o = triple or melting point of pure argon

X_ℓ - mole fraction of argon in the liquid phase

T = triple point of the solution

R = universal gas constant

Equation 6-7 is valid providing three conditions are met. First, the solution must obey Raoult's Law and, second, the solid formed must be pure argon. In view of the previous discussion, the first condition is met, and since solids formed at or near the triple point of pure argon, the second condition is undoubtedly also met. The third condition or restriction is that Equation 6-7 applies only to constant pressure conditions. The pressure coefficient of the logarithm of the equilibrium mole fraction is given by

$$\left(\frac{\partial \ln X}{\partial P}\right)_T = \frac{V_s - V_L}{RT} \tag{6-8}$$

where V_s and V_L = mole volumes of the solid and liquid, respectively
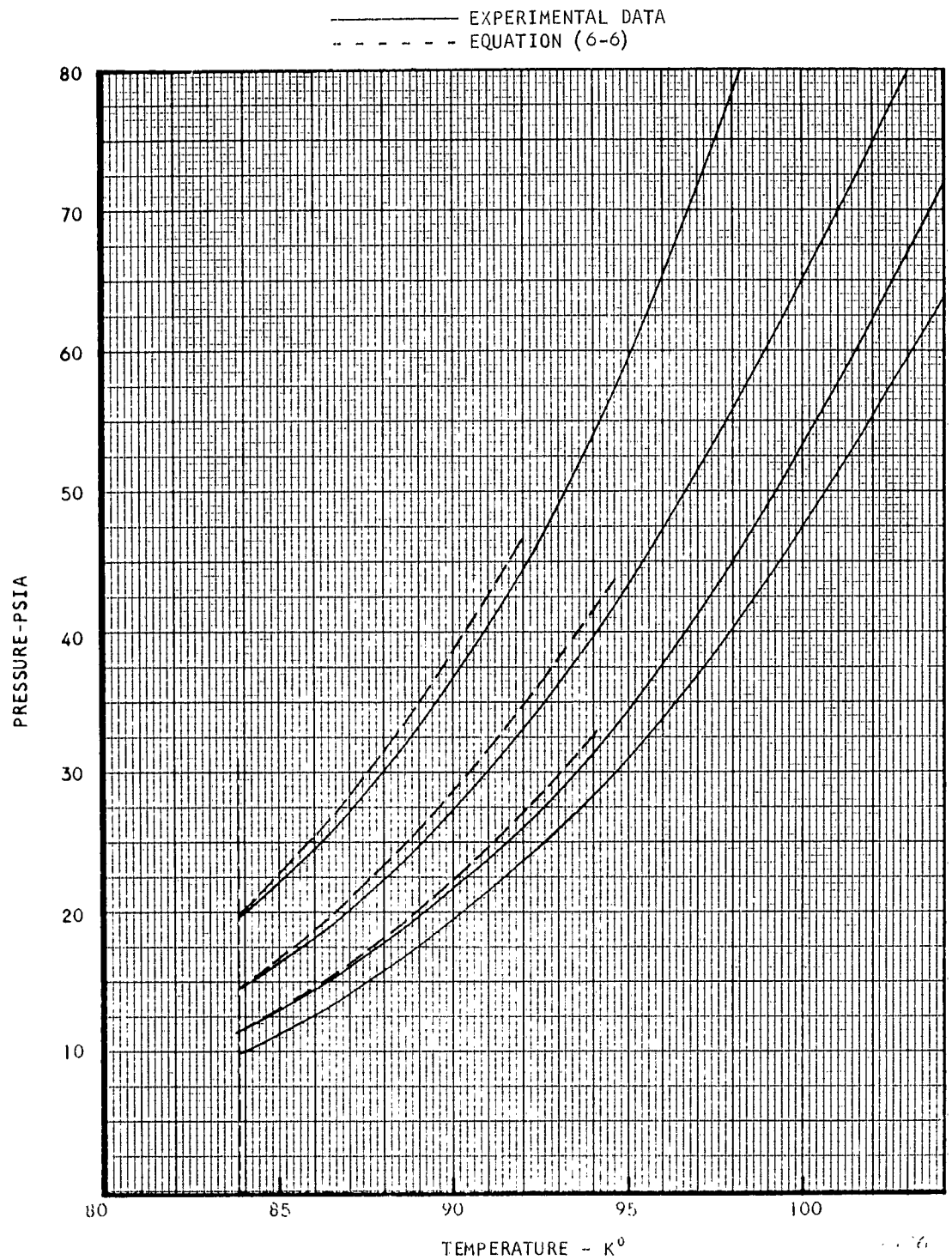
Figure 6-7. Solubility Approximation

In general, the value of the pressure coefficient is very small and the effect of small pressure changes can be neglected. For example, the value of $(\frac{\partial \ln X}{\partial P})_T$ at $83.85^\circ K$ is -4.13×10^{-5} in.^{2}/lb-ft. Equation 6-7 is therefore a good approximation over a moderate pressure range.

Taking the results of Curve 4, Figure 6-5, which represent the maximum neon concentration investigated, the composition of the liquid phase at the intersection of the dew point curve with the solid-vapor boundary can be closely approximated by Equation 6-5.

Thus,

$$X_\ell = \frac{Y\,P_T}{P_\ell} = \frac{(0.5003)\,(19.75)}{9.90} = 0.9975$$

Substitution of this value of X_ℓ into Equation 6-7 yields a triple-point depression of $0.13^\circ K$. Obviously, a slight change in either the mole fraction or the ratio of total pressure to the vapor pressure changes the results radically. For example, the variation of P_T and P_ℓ, within the limits of experimental accuracy, changes the calculated triple-point depression between the limits of zero and $0.8^\circ K$. It was therefore concluded that the actual triple-point depression was less than $0.1^\circ K$ and could not be detected.

Because of the slight solubility of neon in argon, it is unlikely that temperatures along the three-phase line would deviate much from the triple point of pure argon, except possibly at high pressures where an appreciable amount of neon could be forced into solution. Even under these conditions, there is a counteracting effect due to the difference in densities between liquid and solid phases that tends to increase the temperature at which solidification occurs. In any case, the pressures involved would be outside the range of interest in refrigeration applications.

Mixtures of Argon and Nitrogen

The binary mixture system of argon-nitrogen has been partially investigated. Cook[44] gives an up-to-date account of the experimental work done on this system, along with much of the data of the original investigators. This reference lists solid-liquid and vapor-liquid equilibrium data, but does not include solid-vapor or three-phase data. A cursory literature search failed to substantiate the existence of data on these phase boundaries.

40

The liquid-solid data of Long and DiPaolo[45] indicates that substantial three-phase point depressions would be observed in mixtures of argon and nitrogen. For this reason, investigation of the argon-nitrogen triple-point curve appeared desirable. This investigation was undertaken in the final days available for testing under the present contract and, therefore, was limited to investigation of only one mixture. The phase diagram of this mixture (43.17 ± 0.05 percent nitrogen in argon) is presented in Figure 6-8.

Figure 6-9 is a comparison of the bubble point curve of Figure 6-8 with Equation 6-9, which is given by References 44 and 46.

$$\log_{10} P_{atm} = a - \frac{b}{T} \tag{6-9}$$

Equation 6-9 gives the vapor pressure of the liquid phase of argon-nitrogen mixtures as a function of its temperature and the constants a and b. The constants a and b were obtained from plots[44] which give a and b as functions of the liquid phase composition. The solid curve and the dashed curve (Figure 6-9) represent the experimental data and Equation 6-9, respectively. The deviation is within the experimental accuracy over most of the range covered. The larger deviations over part of the range can in part be attributed to errors in obtaining the exact values of the constant a and b from the referenced plots. In addition, the plots of these constants are apparently based on data at a slightly higher temperature and pressure range. The deviation is therefore not considered too serious.

The triple-point or three-phase line in Figure 6-8 extends between the limits of 68.97 ±0.1 °K and 2.74 ±0.1 psia to 68.82 ±0.1 °K and 2.90 ±0.1 psia. The triple point of pure argon is 83.77°K; thus, a triple-point depression of approximately 15°K (27°R) was observed.

The upper end of the three-phase line, pressure-wise, is the end point of the solid-liquid and liquid phase boundary or the liquidus point. Comparing this point with the data of Long and DiPaolo[45], as presented by Cook[44], the agreement is within the accuracy with which the plot presented can be interpreted.
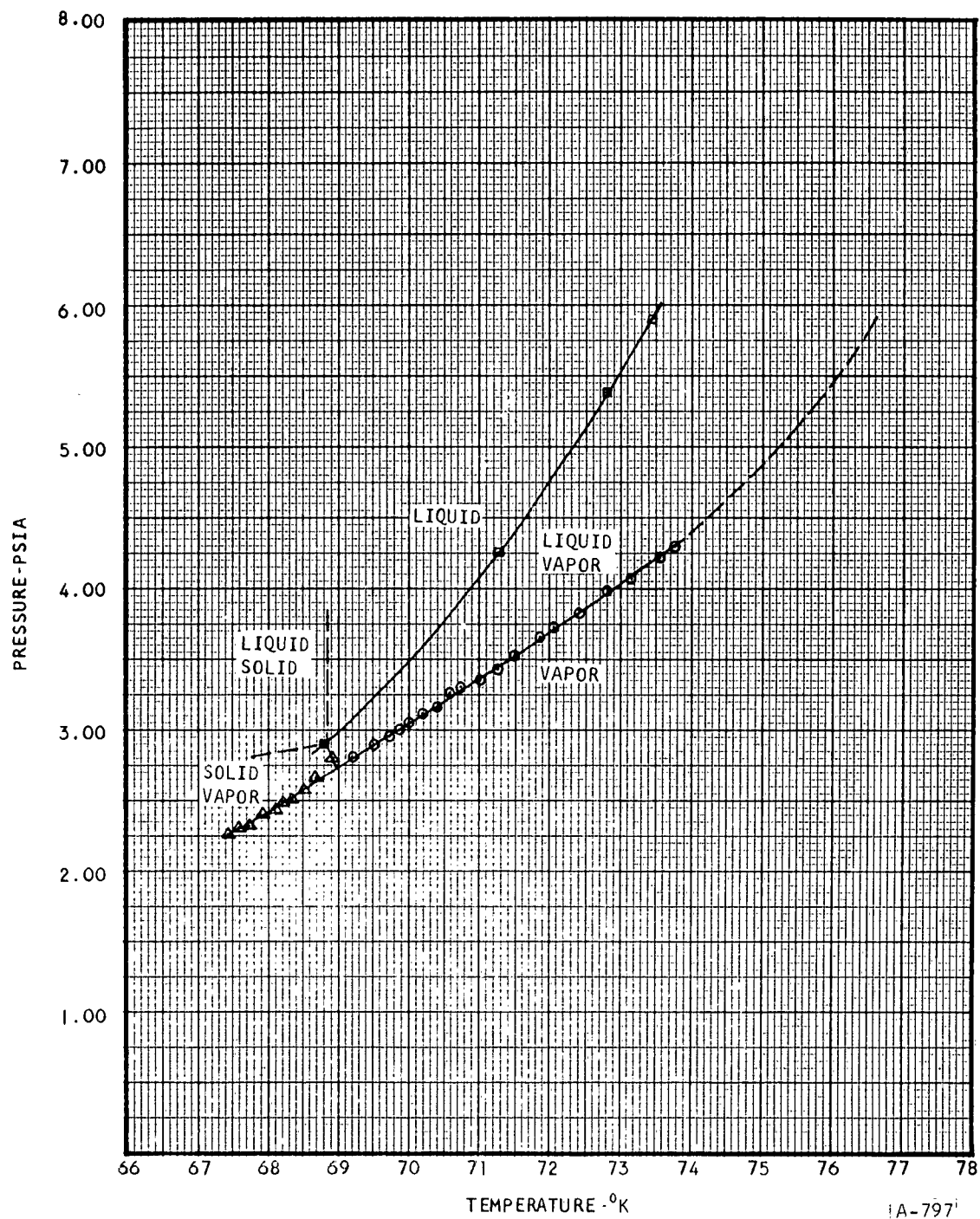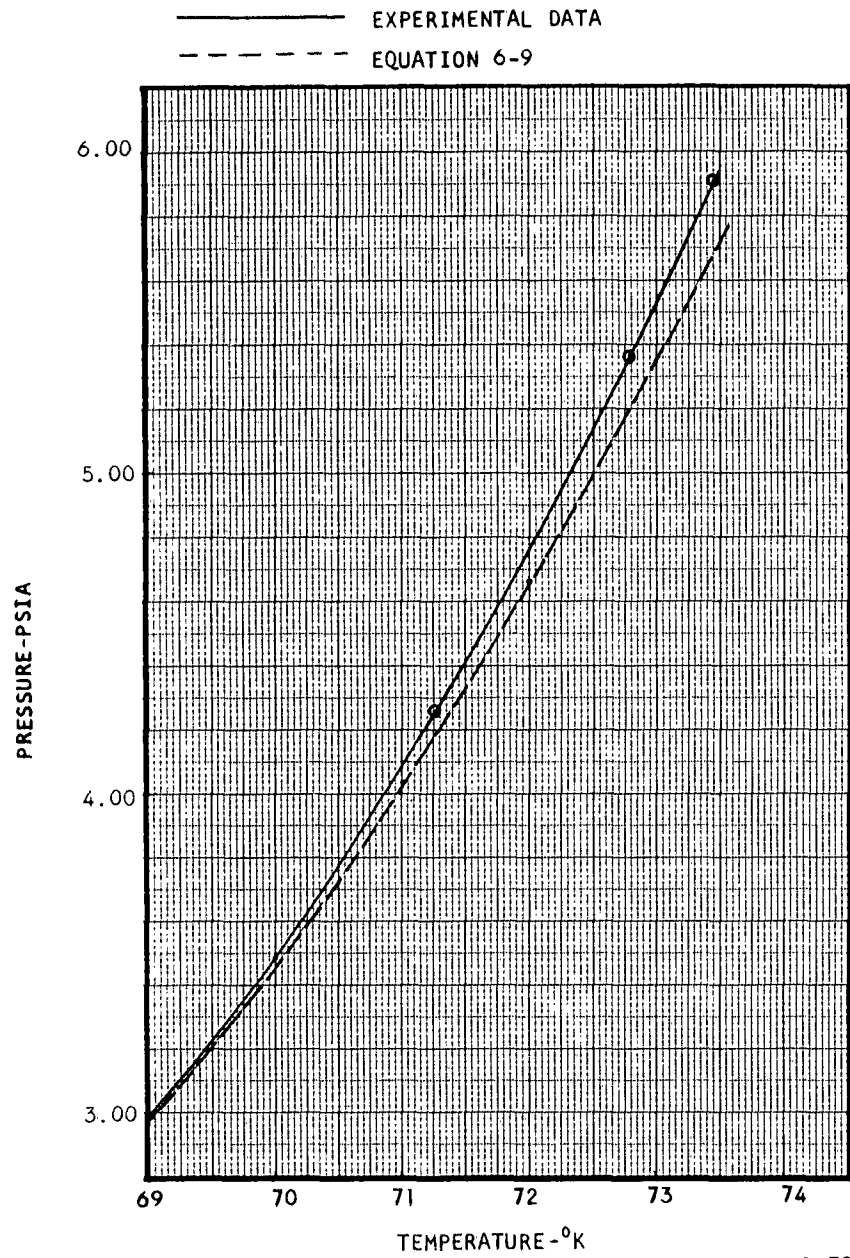
Figure 6-8. Phase Boundaries for 43.17 Percent Nitrogen in Argon

Figure 6-9. Bubble Point Comparison

43

Long and DiPaolo[45] observed two separate solid phases or solid solutions, one of which they designate as α and the other β. There is a miscibility gap where both phases exist between 54.4 to 69.6 percent nitrogen. At lower concentrations of nitrogen, such as the mixture of Figure 6-8, only the α solid solution can coexist in equilibrium with the liquid phase.

In the case of neon-argon mixtures, the triple-point depression was found to be very small. This small triple-point depression indicates that pure argon crystallizes out of the argon-rich liquid in a manner analogous to the crystallization of pure ice (water) from salt solutions. In view of Long and DiPaolo's data, it is of interest to conduct an analysis to determine whether or not the large triple-point depression observed for the nitrogen-argon system can be attributed to the formation of a solid solution.

Considering the case where only one solid solution exists in equilibrium with the liquid phase, the fugacity of the argon in each phase can be equated:

Thus,

$$f_\ell = f_s \qquad (6\text{-}10)$$

where f_ℓ and f_s = the fugacity of the argon in the liquid and solid phases, respectively

Equation 6-10 can be represented equally well by

$$\phi \, X \, f_\ell = \psi \, Z \, f_s \qquad (6\text{-}11)$$

where ϕ and ψ = the fugacity coefficients of the argon in the liquid and solid phases, respectively

X and Z = the mole fractions of argon in the liquid and solid phases, respectively

f_ℓ and f_s = the fugacity of the pure argon in the liquid and solid phases at the same pressure and temperature

Upon taking the logarithm of Equation 6-11 and differentiating with respect to the temperature, Equation 6-12 results:

$$\left(\frac{\partial \ln \phi}{\partial T}\right)_P + \left(\frac{\partial \ln X}{\partial T}\right)_P + \left(\frac{\partial \ln f_\ell}{\partial T}\right)_P = \left(\frac{\partial \ln \psi}{\partial T}\right)_P + \left(\frac{\partial \ln Z}{\partial T}\right)_P + \left(\frac{\partial \ln f_s}{\partial T}\right)_P$$

$$(6\text{-}12)$$

44

To further reduce Equation 6-12, the relation between the partial molar free energy and the fugacity is operated upon. This relation is to be expressed by

$$\overline{F} - F^0 = RT \ln f \tag{6-13}$$

where $\overline{F}$ = the partial molar free energy of the argon

         F^0 = the partial molar free energy at the standard state (i.e., $f_o = 1$)

         R = the universal gas constant

Dividing Equation 6-13 by the temperature and forming the partial derivative with respect to the temperature results in

$$\left[\frac{\partial \left(\frac{\overline{F}}{T} \right)}{\partial T} \right]_P - \left[\frac{\partial \left(\frac{F^0}{T} \right)}{\partial T} \right]_P = R \left(\frac{\partial \ln f}{\partial T} \right)_P \tag{6-14}$$

The Gibbs-Helmholtz equation gives the additional required relationship:

$$\left[\frac{\partial \left(\frac{F}{T} \right)}{\partial T} \right]_P = \frac{H}{T^2} \tag{6-15}$$

In this equation, H = molar enthalpy of argon at P and T. The substitution of Equation 6-15 into Equation 6-14 yields an expression for the temperature coefficient of the fugacity.

$$\left(\frac{\partial \ln f}{\partial T} \right)_P = \frac{H^0 - \overline{H}}{RT^2} \tag{6-16}$$

Equation 6-16 can then be written for each phase as

$$\left(\frac{\partial \ln f_\ell}{\partial T} \right)_P = \frac{H^0 - \overline{H}}{RT^2} \tag{6-17}$$

$$\left(\frac{\partial \ln f_s}{\partial T} \right)_P = \frac{H^0 - \overline{H}_s}{RT^2} \tag{6-18}$$

which, upon substitution into Equation 6-12 and integration, yields

$$\ln \frac{X}{Z} + \ln \frac{\phi}{\psi} = \frac{\overline{\Delta H}_f}{R} \left(\frac{1}{T_o} - \frac{1}{T} \right) \tag{6-19}$$

45

where $\overline{\Delta H}_f$ = the heat of fusion of argon

T_o = the triple point of argon

T = the triple point of the mixture

If the liquid and solid phases are ideal (i.e., ϕ and $\psi = 1$), Equation 6-19 reduces to

$$\ln \frac{X}{Z} = \frac{\overline{\Delta H}_f}{R} \left(\frac{1}{T_o} - \frac{1}{T} \right) \tag{6-20}$$

which, upon letting $Z = 1$, reduces to Equation 6-7 previously used.

Equation 6-20 can be utilized to examine the effect of the formation of a solid solution on the triple point of an ideal system in the following manner. At a constant liquid phase composition (i.e., X is constant), the maximum difference between T and T_o occurs when $Z = 1$. Thus, in this particular case, the effect of the solid solutions is to increase the triple point of the mixture over that which would be expected had the pure solid formed.

In general, the assumption of ideal behavior in the liquid and solid phases is a poor approximation, and experimental determinations are indispensable. In addition, when solid solutions are formed, an additional variable is introduced with results in a greater dependency on experimental data. For example, even though composition of the liquid phase may be known, unless the composition of the coexisting solid solution is also known the triple point cannot be approximated by Equation 6-20.

The main purpose in performing analysis based on ideal behavior is to form a basis for comparison. For example, the measured triple point of the mixture presented in Figure 6-8 is 68.8°K. The solid phase composition calculated by substituting this triple point and the known liquid composition into Equation 6-20 is 80 percent argon. From the plot of Long and DiPaolo, the solid phase composition is approximately 84 percent argon. The close agreement is surprising in that few solid solution-liquid systems behave this ideally. In general, the ratio, or the absolute value, of the fugacity coefficients ϕ and ψ does not approach one, and Equation 6-19 plus the measured coefficients are required to describe the behavior.

SECTION 7

APPLICABILITY AND FEASIBILITY OF UTILIZING BINARY GAS MIXTURES
AS CLOSED-CYCLE CRYOGENIC REFRIGERANTS

The purpose of this section is to discuss the various problem areas and possible advantages of utilizing binary gas mixtures as cryogenic refrigerants.

CRITERIA FOR APPLICABILITY

The three major criteria for selection of a cryogenic refrigerant for use in a closed-cycle system are as follows:

1. The phase boundaries must be compatible with the temperature and pressure range covered by the particular cycle under consideration.

2. The refrigerant must exhibit thermodynamic properties favorable to the use of an efficient thermodynamic cycle in the temperature range required.

3. The physical properties of the refrigerant must be compatible with the mechanical design of practical systems.

In particular, for a binary gas mixture to be of value as a cryogenic refrigerant, it must fulfill at least one of these criteria where the pure gases utilized at present either partially or totally fail. The pure gases exhibit weaknesses in all three of the above criteria under various conditions. For example, the fixed phase boundaries of pure gases impose severe limitations on the refrigeration temperature range that can be covered by vapor-liquid cycles. The low molecular weights of gases such as helium and hydrogen result in large power requirements for compression in either gas or vapor-liquid cycles. In addition, the behavior of the heat capacity property of gases at low temperatures often complicates the design of effective heat exchangers. In the following paragraphs, the possibility of the judicious utilization of binary gas mixtures to improve cryogenic refrigeration performance will be analyzed.

47

LIMITATIONS IMPOSED BY PHASE BOUNDARIES

The phase boundaries of the refrigerant limit the temperature and pressure range in which a given cycle can operate. For example, a vapor-liquid cycle such as the Claude cycle must operate with its evaporator at conditions within the vapor-liquid phase boundaries. In a like manner, gas cycles such as the reversed Brayton and Stirling cycles must operate outside of the vapor-liquid boundary.

Vapor-Liquid Cycles

In the case of vapor-liquid cycles, the use of pure gases as refrigerants limits the operating or refrigeration temperature to a narrow range near the normal boiling point, with the triple point as the lower limit and the critical point as the absolute upper limit.

If gas mixtures can be found that exhibit vapor-liquid equilibrium at temperatures intermediate between the boiling points of the elementary gases, a possible means of extending the temperature range covered by vapor-liquid cycles exists. A prime goal of this study has been to establish the temperature range over which the liquid phase of each of the selected mixtures can coexist in equilibrium with the vapor phase.

At a given pressure, a complete range of boiling points between those of the pure components would be expected in the case of normal binary mixtures. This behavior was not anticipated with mixtures of the cryogens. Each of the cryogens considered in this program is characterized by having its boiling point and triple point not greatly removed from one another on the temperature scale. In all the systems selected for study, the boiling point of the lighter component is lower than the triple point of the heavier component. Thus, the solid phase may appear as the temperature of the mixture is lowered toward the boiling point, below the triple point of the heavier component. It thus becomes evident that the possibility of extending the refrigeration temperature range covered by vapor-liquid cycles, by utilizing binary mixtures, is dependent on the triple or three-phase point of the mixture.

The triple point of a mixture is not uniquely defined as it is for a pure component. Instead, there is a locus of triple or three-phase points defined

by the pressure and composition, with one degree of freedom in accordance with the Gibbs Phase Rule. This is clearly seen in Figure 6-4, where the three-phase line extends from the intersection of the vapor-solid and vapor-liquid boundaries to the intersection of the liquid-solid and liquid-phase boundaries.

The binary systems initially selected for study are as follows:

Neon-Argon
Neon-Nitrogen
Neon-Hydrogen
Neon-Helium
Hydrogen-Nitrogen

Of these systems, only that of neon-argon was investigated experimentally. Four different mixtures of this system were investigated, and no measurable change in the three-phase temperature from that of pure argon was observed. An analysis was conducted which confirmed the conclusion that appreciable triple-point depressions would not occur within the pressure range of interest in refrigeration applications for this combination; the results of this analysis are presented in Section 6.

The behavior of the neon-argon system can be used to gain some insight into what might be expected of similar systems. The critical temperature of neon is below the boiling or triple point of argon. It is shown in Section 6 that neon is only slightly soluble in the condensed phase at moderate pressures. This slight solubility is mainly attributed to the fact that the condensed or liquid phase of pure neon cannot exist at temperatures over its critical temperature. Excessive pressures would therefore be required to force the neon into solution and lower the triple point in accordance with Equation 6-7.

The systems selected for study can be categorized according to whether or not the critical temperature of the lighter component is below the triple point of the heavier component. Referring to Table 7-1, it is found that neon-helium, neon-nitrogen, and hydrogen-nitrogen fall into the same category as the neon-argon system investigated, whereas neon-hydrogen does not. It is therefore anticipated that large triple-point depressions would not be observed in the first three systems above.

TABLE 7-1

PHASE TRANSITION TEMPERATURE COMPARISON

Gas	Boiling Point ^{o}K	Triple Point ^{o}K	Critical Temperature ^{o}K
Helium	4.216	--	5.22
Hydrogen	20.39	13.96	33.22
Neon	27.1	24.57	44.39
Nitrogen	77.34	63.15	126.28
Argon	87.29	83.85	150.72

However, insufficient experimental work has been done in this area to establish a definite correlation. Therefore, each of the systems, neon-helium, neon-nitrogen, and hydrogen-nitrogen, warrants at least a probing investigation in the future. In particular, the system of neon-helium appears promising. The triple point of neon is not so widely removed from the critical point of helium that an appreciable amount of helium could not dissolve in the liquid phase.

The system of neon-hydrogen can be compared with that of argon-nitrogen. In both cases, the boiling points of the components are not widely separated and the triple point of the heavier component is below the critical temperature of the lighter component.

One mixture of the system of nitrogen-argon was investigated experimentally. In this case, a substantial triple-point depression was observed. It is likely that the system of neon-hydrogen would exhibit this same type of behavior.

In the case of either nitrogen-argon or hydrogen-neon, the net result of substantial triple-point depressions, below that of the heavier component, cannot be considered to extend the temperature range covered by vapor-liquid cycles, since the same temperature range could be covered by the lighter component in each case. There are, however, other possible advantages such as better thermal-physical properties of the mixtures which could make their utilization advantageous.

Gas Cycles

Thermodynamic cycles such as the Stirling and reversed Brayton cycles are designed to operate entirely in the gas phase. This design restriction is due to the impracticability of developing long-life rotary or reciprocating machinery to operate in the two-phase region. Thus, where it is the three-phase line that imposes the lower refrigeration temperature limit on vapor-liquid cycles, the vapor dome or dew-point curve sets a similar limit on gas cycles for a particular working fluid.

In the past year, a great deal of interest has been shown in the reversed Brayton cycle as a means of providing refrigeration at cryogenic temperatures. In view of this renewed interest, the reversed Brayton cycle will be used to illustrate the possible application of binary mixtures to gas cycles. In general, the same arguments apply to all gas cycles.

Figure 7-1 presents an equipment schematic and the temperature-entropy diagram of a typical reversed Brayton cycle for aerospace applications. Referring to Figure 7-1, the operation of the cycle is as follows: The gas is compressed and then cooled from points 5 to 1 by means of the compressor and space radiator. The high-pressure gas is then cooled from points 1 to 2 in the regenerative heat exchanger, where it gives up energy to the low-pressure gas returning from the refrigeration load. The high-pressure vapor is then expanded in the turboexpander as shown by process 2-3, with a consequent reduction in temperature level. The gas then enters the cooling load heat exchanger, where it experiences sensible heating as it absorbs the refrigeration heat load, as indicated by process 3-4. The gas then passes through the low-pressure side of the regenerative heat exchanger (process 4-5) to complete the cycle.

For a particular application, a refrigeration temperature below that of T_{ref} shown in Figure 7-1 may be required. To avoid contacting the vapor dome or two-phase region, the location of the cycle relative to the vapor dome must be changed. Figure 7-2 shows three different possible solutions to achieve a lower refrigeration temperature.

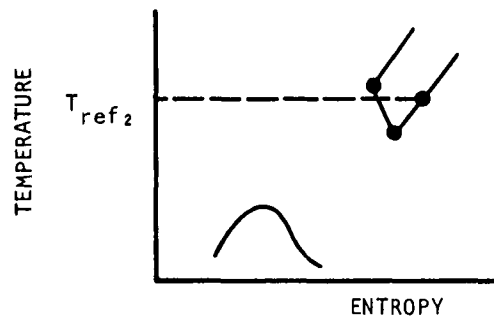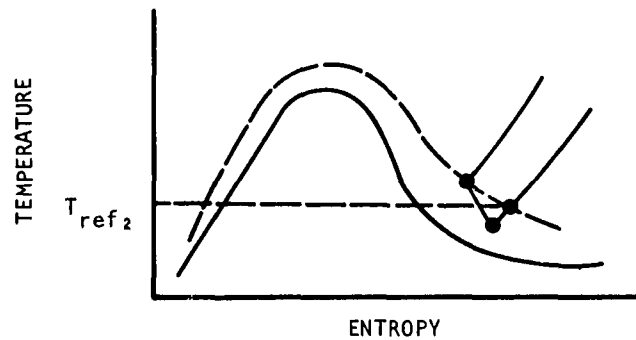Figure 7-1. Reversed Brayton Refrigeration Cycle
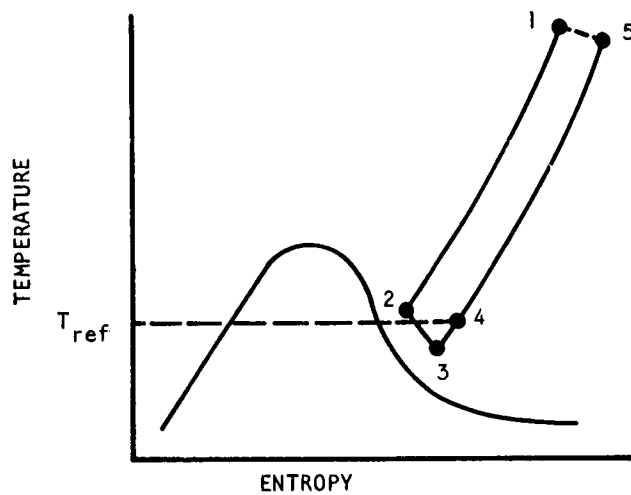
(a)   LOWER REFRIGERATION TEMPERATURE BY
      OPERATING AT LOWER PRESSURE LEVELS
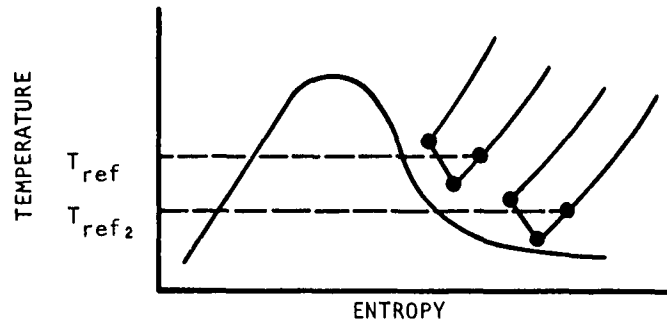
(b)   LOWER REFRIGERATION TEMPERATURE BY CHANGING
      TO LOWER-MOLECULAR-WEIGHT PURE GAS

(c) - LOWER REFRIGERATION TEMPERATURE BY
         UTILIZING A GAS MIXTURE

A-800

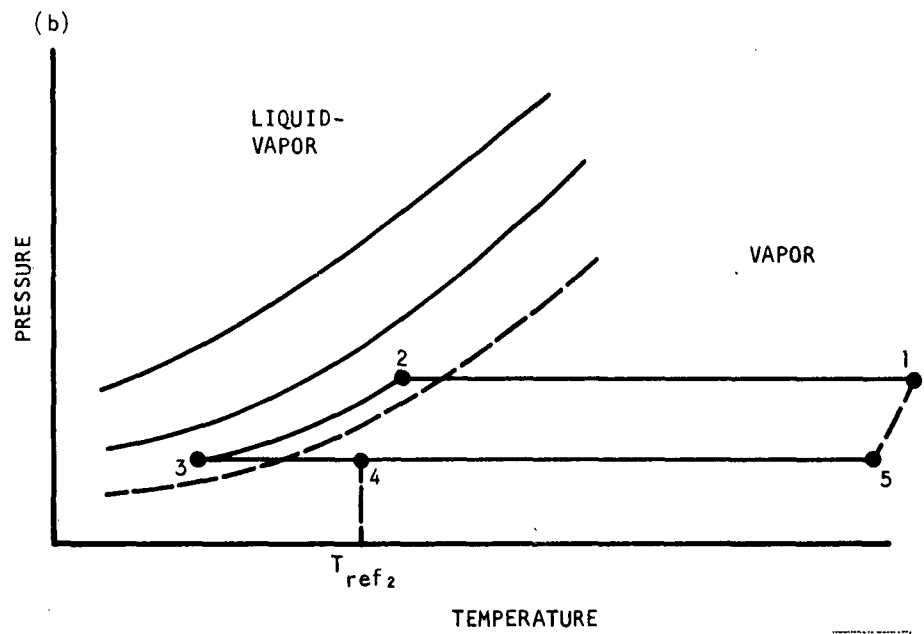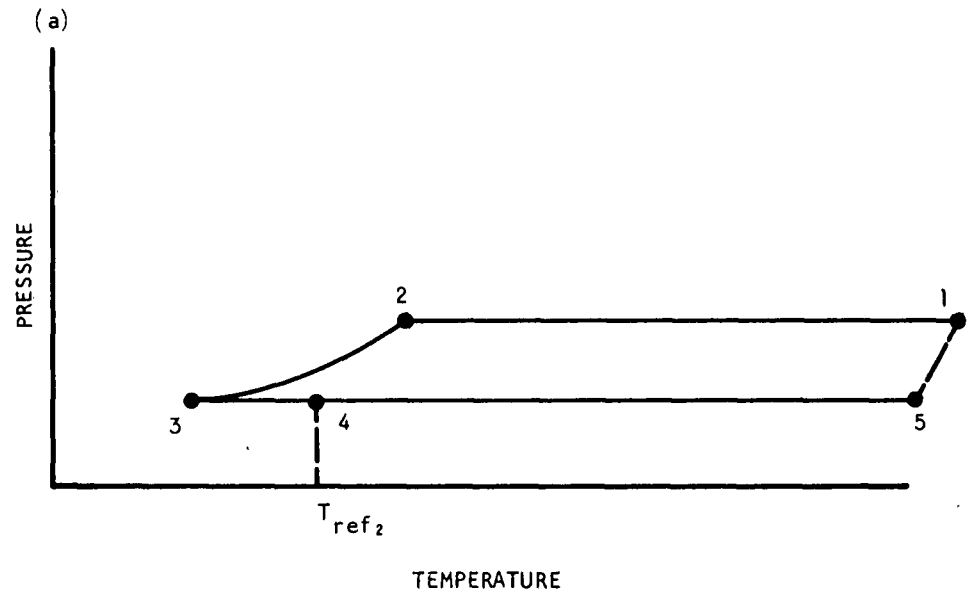Figure 7-2.   Reversed Brayton Cycle Comparison

53

In Figure 7-2(a), the lower refrigeration temperature T_{ref_2} is reached by operating in the low-density region of the same gas represented by the temperature-entropy diagram in Figure 7-1. In some cases, depending on the requirements of the particular application, operating in the low-density region is satisfactory. However, in general, the size of the equipment gets larger as the pressure level is lowered and an optimum system may not be obtained.

In Figure 7-2(b), the lower refrigeration temperature T_{ref_2} is obtained by utilizing a lower-molecular-weight gas as a refrigerant. Utilization of low-molecular-weight gases imposes practical limitations on the design of various components of the system. For example, the molecular weight of the refrigerant is of particular importance in refrigeration systems utilizing turbomachinery. With this type of equipment, the number of stages required in the compressor can be reduced by using high-molecular-weight refrigerants.

In Figure 7-2(c), the lower refrigeration temperature T_{ref_2} is obtained by utilizing a hypothetical binary mixture. The dashed vapor-dome in Figure 7-2(c) represents the pure gas in Figure 7-2(a). The solid vapor-dome in Figure 7-2(c) can be considered as a binary mixture of this gas with that of Figure 7-2(b).

The disadvantages of obtaining a lower refrigeration temperature by the methods of Figures 7-2(a) and 7-2(b) are at least partly overcome by utilizing the mixture. First, the cycle can now be operated in a higher density range, which enables the design of compact components. Second, the molecular weight of the mixture is much higher than that of the lighter pure gas. Thus, the limitations on compressor design are reduced. In a subsequent discussion, the effect of the molecular weight will be more fully analyzed.

To more clearly illustrate how the data of Section 6 can be used, Figure 7-3 was drawn. Figure 7-3(a) presents a reversed Brayton cycle on a pressure-temperature diagram. Figure 7-3(b) presents the same cycle superimposed on a set of dew-point curves similar to those presented in Figure 6-5. The dashed dew-point curve can be considered as a pure gas and the solid curves represent mixtures of progressively higher concentrations of the lighter component.

(a)

PRESSURE

2   1

3   4   5

T_{ref_2}

TEMPERATURE

(b)

LIQUID-
VAPOR

VAPOR

PRESSURE

2   1

3   4   5

T_{ref_2}

TEMPERATURE

A-801

Figure 7-3. Reversed Brayton Cycle Comparison

55

It is obvious that the cycle will not clear the two-phase region if the pure heavy component of the mixture is used. However, by adjusting the composition of the mixture, operation at the desired pressure and temperature level is possible. It appears from the data of Figure 6-5 and Figure 6-8 that a more pronounced movement of the vapor dome is effected when the boiling points of the pure components are widely separated. Thus, systems such as neon-argon, hydrogen-nitrogen, neon-nitrogen, and the combinations of helium with heavier components appear most promising for application to gas cycles.

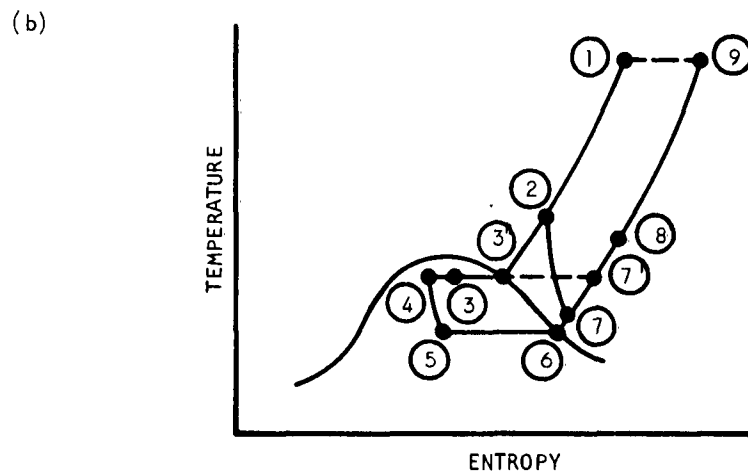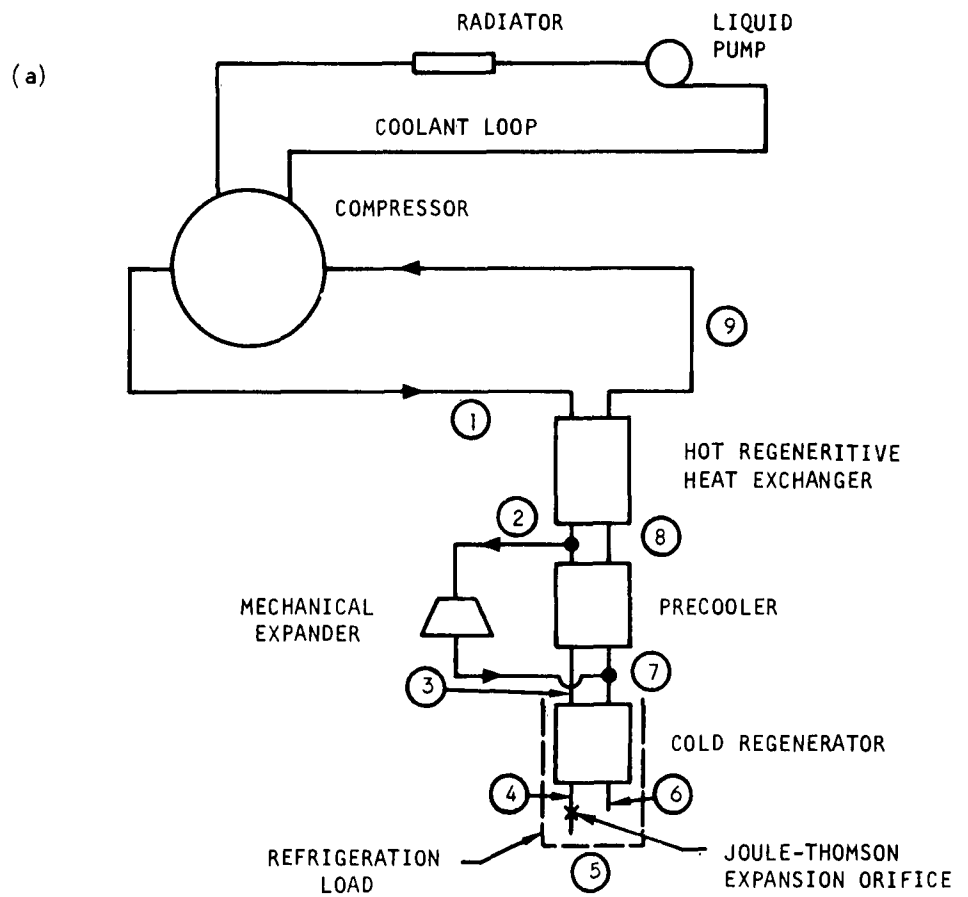EFFECT OF PHASE BEHAVIOR ON THERMODYNAMIC CYCLES

A system composed of two or more components exhibits a more complex phase behavior than is found in the case of a pure substance. The following discussion will be devoted to pointing out a few of the major effects of the phase behavior of binary mixtures on the thermodynamic cycles of typical refrigeration systems.

Liquid-Vapor Cycles

The Claude vapor-liquid cycle is used as an example for the subsequent discussion.

Figure 7-4 represents a Claude bypass expander system. The bypass expander system is shown schematically in Figure 7-4(a), and the working fluid thermodynamic cycle is traced in Figure 7-4(b).

Referring to Figure 7-4, operation of the cycle is as follows: The high-pressure gas discharged from the compressor (1) flows through the hot regenerative heat exchanger, the precooler, and the cold regenerator in series as indicated by the processes (1)-(2), (2)-(3), and (3)-(4). The working fluid is cooled in these three heat exchangers and partly liquefied before being expanded isenthalpically through an orifice, process (4)-(5). The liquid thus produced provides the refrigeration by giving up its latent heat of vaporization as shown by process (5)-(6). The saturated vapor at (6) is then passed through the three heat exchangers, where it cools the incoming gas as indicated by the processes (6)-(7), (7)-(8), and (8)-(9). A portion of the high-pressure gas from the cold end of the hot regenerative heat

56

(a)

RADIATOR

LIQUID PUMP

COOLANT LOOP

COMPRESSOR

⑨

①

HOT REGENERITIVE HEAT EXCHANGER

②

⑧

MECHANICAL EXPANDER

PRECOOLER

③

⑦

COLD REGENERATOR

④

⑥

REFRIGERATION LOAD

JOULE-THOMSON EXPANSION ORIFICE

⑤

(b)

TEMPERATURE

ENTROPY

[A-802]

Figure 7-4. Claude Bypass Expander System

57

exchanger is tapped off and cooled to a relatively low temperature by expansion in a work-extraction device, process (2)-(7). The exhaust from the expander re-enters the cycle between the cold regenerator and the precooler, mixing with the gas exhausted from the refrigeration load. By increasing the flow in the expander relative to the flow through the Joule-Thomson expansion orifice, a high degree of precooling can be achieved, and condensation of the working fluid can be obtained in the precooler as well as in the cold regenerator. Full advantage is thus taken of the cooling capacity of the expander. No liquefaction occurs in the expander, although the gas exhausts from it at a temperature lower than the dew point of the working fluid at the high-pressure level.

Figure 7-5 represents a Claude cycle utilizing a hypothetical binary mixture. The general behavior of that part of the cycle which is above the vapor dome is unchanged from that shown in Figure 7-4(b). The processes within the vapor dome are, however, affected in the following manner. In Figure 7-4(b), processes (3)-(4) and (5)-(6) are both isothermal and isobaric in accordance with the phase behavior of a pure component. In Figure 7-5, processes (3)-(4) and (5)-(6) are isobaric but not isothermal. This behavior is due to the characteristic phase relations of binary mixtures. That is, in accordance with Gibbs' Phase Rule, there is one more degree of freedom in the two-phase region for a binary mixture than a pure substance. Thus, if the pressure is held constant and the relative amounts of the two phases are changed, either by condensation or evaporation, the temperature must change.

In Figure 7-5, the dashed lines extended along the isobars of processes (3)-(4) and (5)-(6) intersect the liquid-vapor dome at the bubble points corresponding to the pressure levels of these processes. This is more clearly seen in Figures 7-6(a) and 7-6(b), which present the dew and bubble point diagrams corresponding to the two pressure levels. In Figure 7-6(a), the gas mixture of composition X is cooled from (2) to (3). At (3) condensation begins. As the mixture is cooled further, the ratio of the mass in the
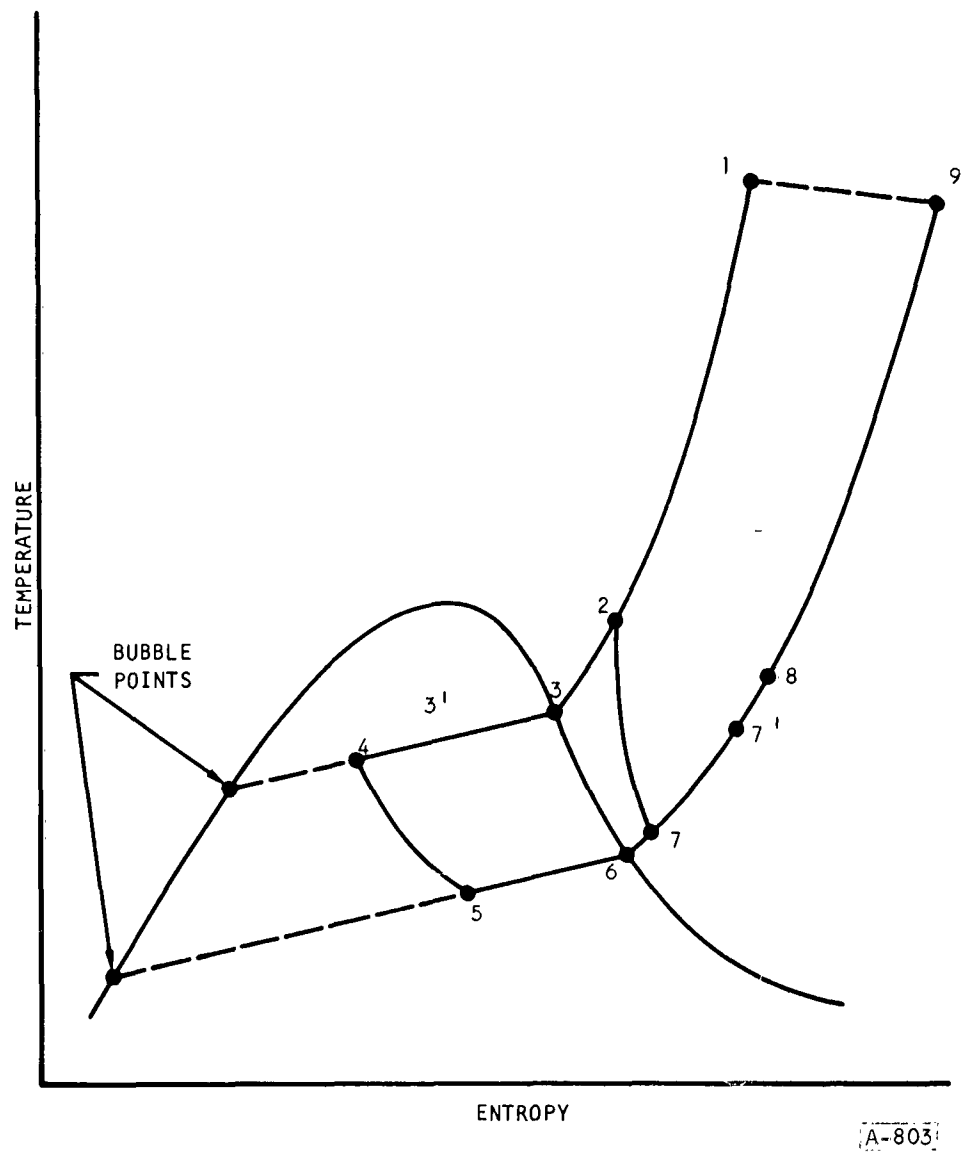
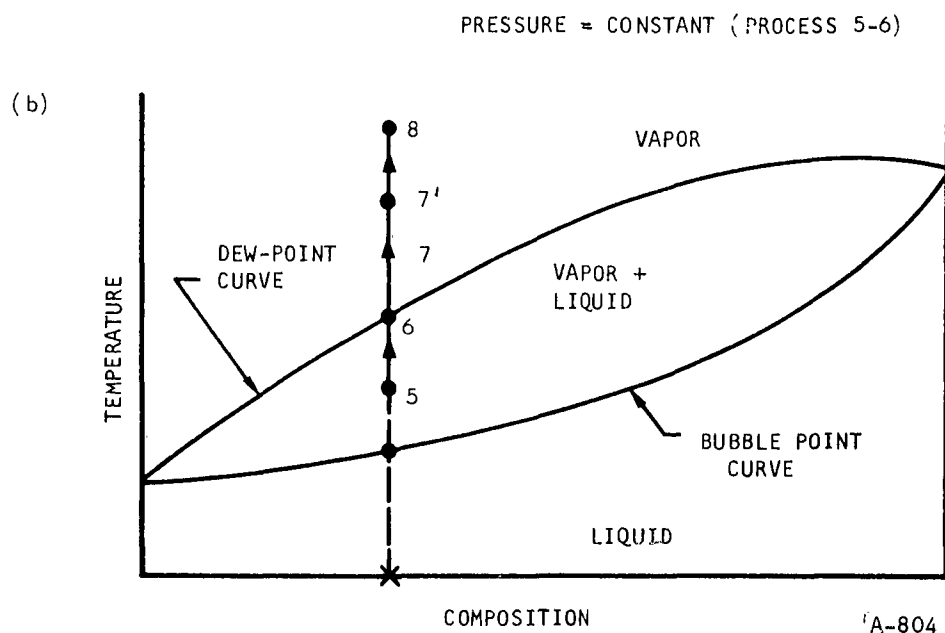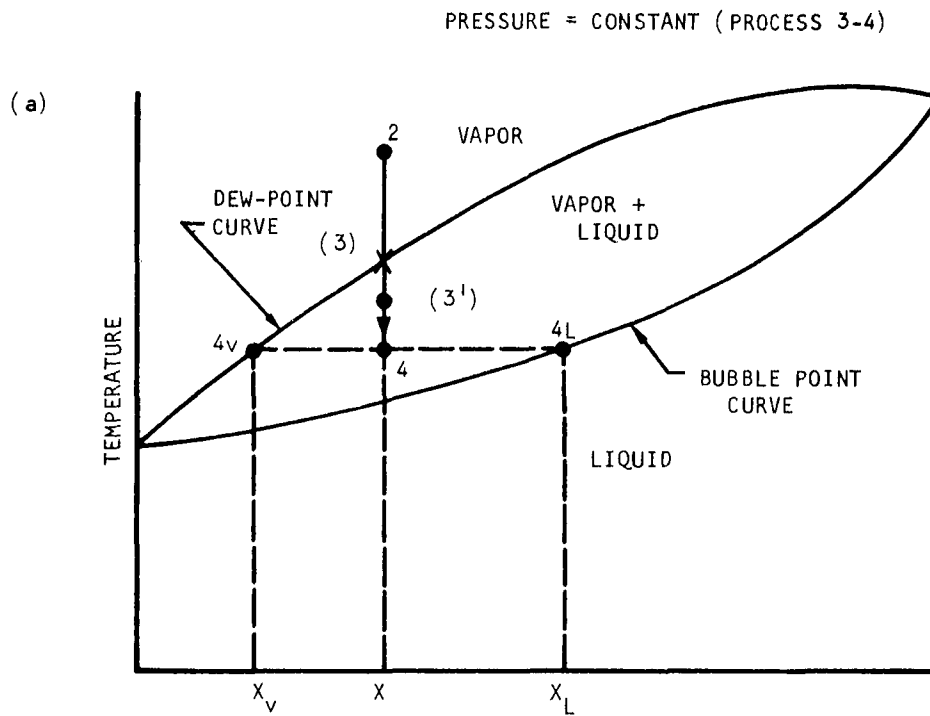Figure 7-5. Claude Cycle Utilizing a Binary Mixture

59

Figure 7-6. Claude Cycle Points on Binary Mixture
Dew and Bubble Point Diagrams

liquid phase to that in the vapor phase increases. For example, at (4) the ratio of the mass in the liquid-to-vapor phase is given by Equation 7-1, the familiar lever rule:

$$\frac{m_L}{m_V} = \frac{X - X_V}{X_L - X} \qquad (7-1)$$

Figure 7-6(b) shows the vaporization process. As the mixture absorbs the refrigeration heat load, the temperature increases. At point (6) the liquid phase is completely gone and the remaining processes are as shown in Figure 7-5.

Figure 7-7 is a comparison of the temperature profiles across the pre-coolers and cold regenerators of the cycles presented in Figures 7-4 and 7-5. This comparison indicates that the use of mixtures produces a more uniform temperature differential from point to point along the length of the heat exchangers. Thus, the amount of heat transferred per unit area is more constant in the case of the mixture. In future designs it may prove possible to take advantage of this behavior to relax heat exchanger designs.

One of the principal advantages of vapor-liquid cycles is the maintenance of a constant temperature in the refrigeration zone. For example, process (5)-(6) in Figure 7-4 is a constant-temperature process. In Figure 7-5, the refrigeration heat load is absorbed over a finite temperature range as shown by process (5)-(6). Thus, one of the main advantages of the cycle is lost when a mixture is used as a refrigerant unless some compensating design factor is introduced.

Figure 7-8 represents a Claude cycle utilizing a binary gas mixture as a working fluid. This cycle is similar to that shown in Figure 7-5 except that a constant-temperature evaporator or refrigeration zone is shown. To

PRECOOLER TEMPERATURE PROFILES

(a) PURE GAS

(b) MIXTURE

COLD REGENERATOR

(c) PURE GAS
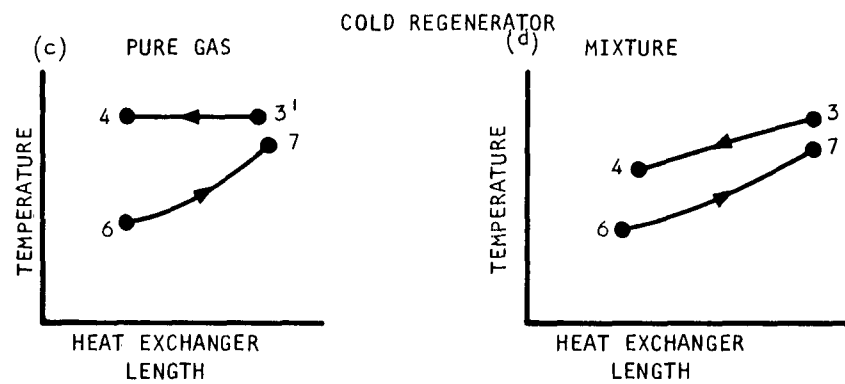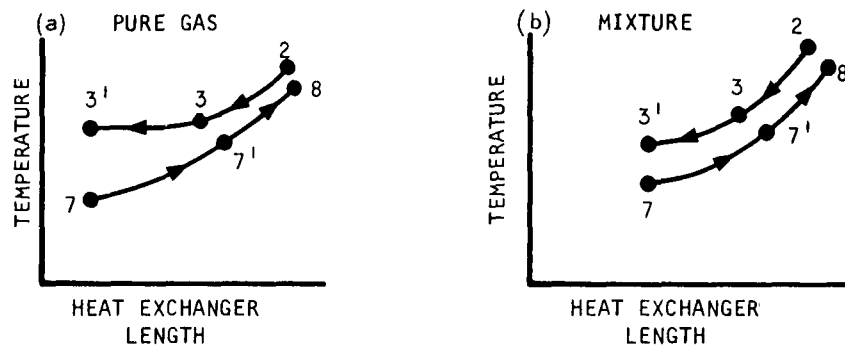
(d) MIXTURE

A-805

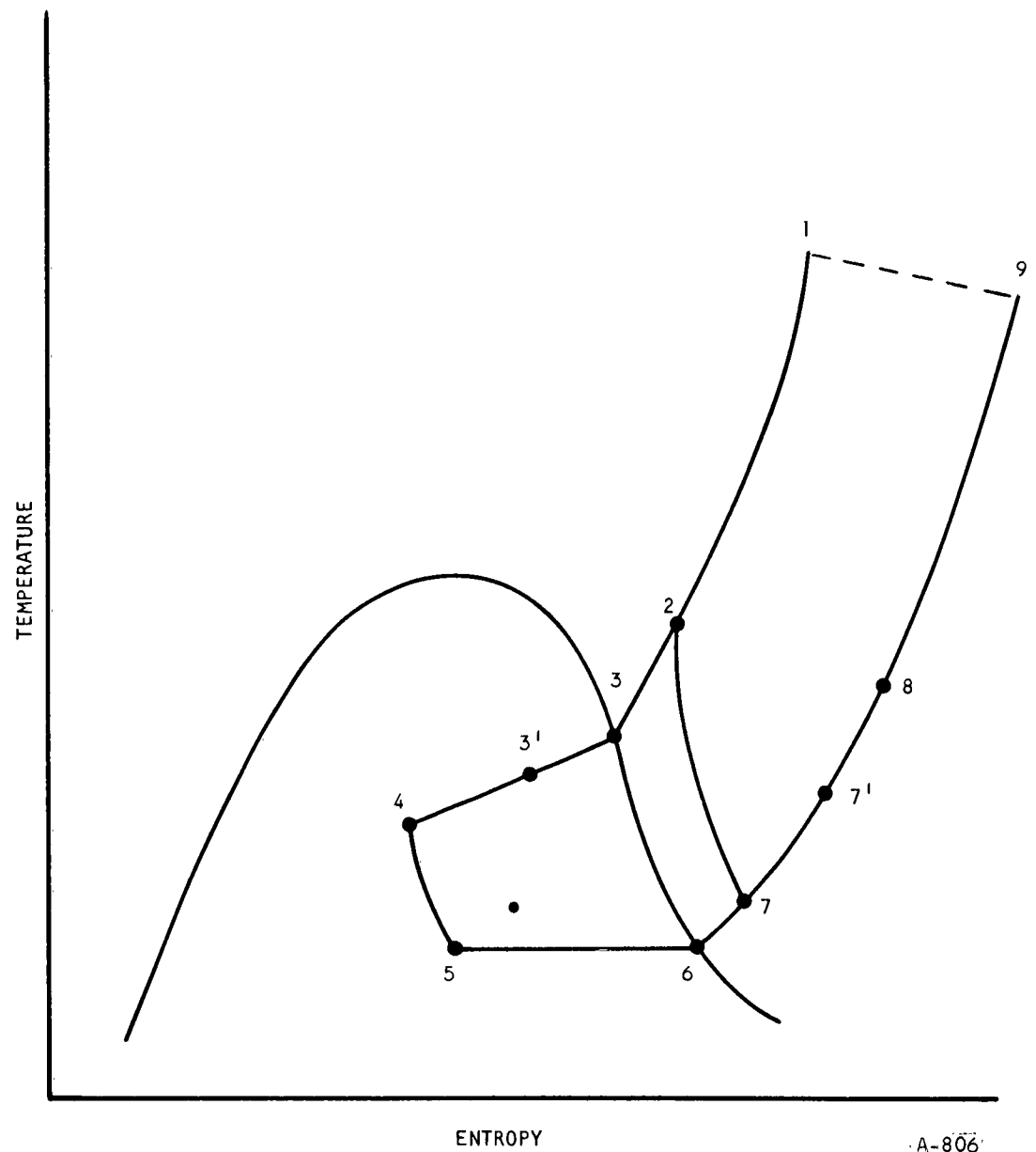Figure 7-7   Heat Exchanger Temperature Profile Comparison

Figure 7-8. Claude Cycle Utilizing a Binary Mixture
with a Constant-Temperature Evaporator

achieve this effect is analogous to designing a constant-temperature distillation column. The process is more clearly seen in Figure 7-9.

Figure 7-9 is a dew and bubble point diagram of the mixture utilized in the cycle shown in Figure 7-8 at the temperature of process (5)-(6). The ratio of the mass of liquid to that of the vapor is again given by Equation 7-1. As the mixture absorbs the refrigeration heat load, the liquid phase is vaporized at constant temperature with a corresponding decrease in the pressure level.

The design of a constant-temperature evaporator for refrigeration systems utilizing binary mixtures is a challenging but not unachievable task. The difficulties arise from the following conditions of constraint which must be satisfied: At every point along the line between (5) and (6) in Figure 7-9, the heat absorbed up to that point must be such as to correspond to the heat required to maintain the ratio of liquid to vapor in accordance with Equation 7-1. In addition, the pressure drop through the evaporator must, point-wise, also correspond to the ratio of liquid to vapor along line (5)-(6). Obviously, the greater the difference between the dew and bubble point pressure at a given temperature, the more difficult the problem becomes and the greater the cycle power penalty becomes.

For constant-temperature evaporation, it is evident that mixtures which exhibit phase behaviors similar to the neon-argon mixture shown in Figure 6-4 are less desirable than mixtures similar to the nitrogen-argon mixture shown in Figure 6-8.

The difference between the dew and bubble point pressures of the neon-argon mixtures is large even though the neon concentration is low. At higher neon concentrations, even larger differences would be observed.

The difference between the dew and bubble point pressures of the nitrogen-argon mixture shown in Figure 6-8 is relatively small. In the low-temperature region near the three-phase line, the dew and bubble point pressure difference is very small. Thus, the development of a refrigeration system, featuring a constant-temperature evaporator operating at temperatures near the three-phase line of this and similar mixtures, is particularly feasible.

TEMPERATURE = CONSTANT (PROCESS (5)-(6))
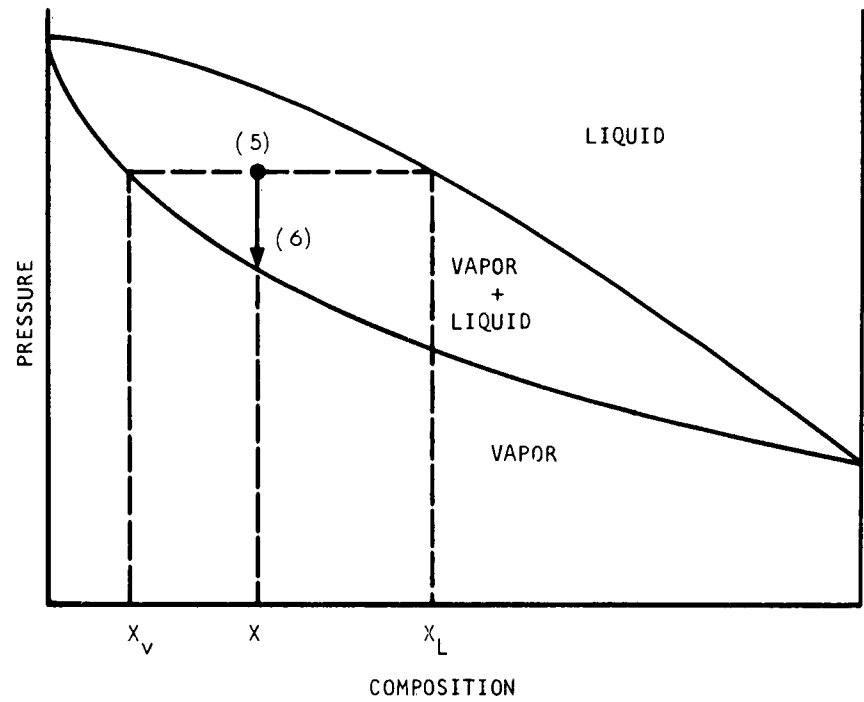
Figure 7-9. Dew and Bubble Point Diagram

Though the previous discussion has made use of the Claude cycle for illustrative purposes, the problems are similar for the other vapor-liquid cycles.

Gas Cycles

In a single-phase region, such as the gas phase, a mixture of constant composition exhibits the same general behavior characteristic of pure substances. Thus, cycles that operate entirely in the gas phase are similar whether a mixture or pure substance is used as a working fluid.

The thermal and physical properties vary from pure gas to pure gas as well as from mixture to mixture. Thus, though the thermodynamic plots of gas cycles for mixtures and pure gases have the same general shape,the efficiencies can vary greatly. In the subsequent paragraphs, the thermal and physical properties of mixtures will be discussed.

SYSTEM SELECTION

To this point, only the limitations imposed by phase boundaries and the effects of phase behavior on various thermodynamic cycles have been discussed. In the final analysis, primary interest is centered in the properties of binary gas mixtures that permit increased refrigeration machine performance. The vistas to be opened by the determination of binary gas mixture properties appear to offer unlimited possibilities for improvement in component and cycle performance and will, undoubtedly, influence the selection of the type of system in many cases.

The selection of a working fluid and a particular type of cycle, for a given application, requires detailed cycle analyses and machinery performance analyses, and comparisons of these analyses to obtain an optimum system. That is, calculations must be made with the cycles and working fluids possible under the limitations imposed by the phase boundaries and machinery characteristics, resulting in the determination of state points comprising the cycles, and permitting comparison of power requirements, refrigeration capacity, and flow rates. Such analyses must examine the effects of the variation of all the parameters involved. Typically, for a given cycle and working fluid, the temperature difference in the heat exchanger or heat exchangers and the efficiencies of the machinery elements would be varied.

The use of mixtures a_ working fluids introduces an additional parameter that could result in a better system for a given application than the optimum system selected from an analysis of pure gas cycles. The iterative nature of the calculations involved in cycle analysis makes it a time-consuming task. In addition, these analyses rely on the knowledge of the thermodynamic and physical properties of the working fluid. Inasmuch as these data are unknown for most mixtures, a complete comparison between cycles utilizing mixtures and those using pure gases cannot be made. However, component performance in many cases is defined in terms of readily determinable gas properties such as molecular weight. It is therefore possible to obtain an indication of the relative performance of components operating with binary refrigerants and components operating with pure gas refrigerants.

Molecular Weight Effects

The molecular weight of a mixture is somewhere between the limits of the molecular weights of the pure components making up the mixture. For example, the molecular weight of a 50-50 mixture of argon (molecular weight = 39.94) and helium (molecular weight = 4.003) is 21.97. Thus, the average molecular weight of this mixture is approximately five times greater than the lighter component and one-half that of the heavier component. In the ideal gas region, the mixture is likewise five times denser than the lighter component and one-half as dense as the heavier component.

The molecular weight of a working fluid has considerable effect on the compression and expansion processes. For an adiabatic compression process, the energy required to increase the pressure of a unit mass of fluid over a given pressure ratio is termed the adiabatic head. This quantity is given by Equation 7-2, where compression takes place in the ideal gas region:

$$H_{ad} = \frac{1}{\eta_c} \left(\frac{\gamma}{\gamma-1}\right) \frac{1545}{M} \left(Pr^{\frac{\gamma-1}{\gamma}} - 1\right) T_{in} \qquad (7-2)$$

where Pr is the pressure ratio, η_c is the compressor adiabatic efficiency, and M and γ are the molecular weight and specific heat ratio, respectively, of the fluid being compressed. T_{in} is the fluid temperature at the compressor inlet.

The adiabatic head is clearly a strong function of the working fluid properties, particularly the molecular weight.

The working fluids being considered for a particular application can be compared by rewriting Equation 7-2, with η_c taken as unity as follows:

$$\frac{H_{ad}}{T_{in}} = \frac{\gamma}{\gamma-1} \left(\frac{1545}{M}\right) \left(Pr^{\frac{\gamma-1}{\gamma}} - 1\right) \qquad (7-3)$$

Figure 7-10 is a comparison of Equation 7-3 for the pure components of the mixtures considered in this study.

The power necessary to carry on an adiabatic compression process is given by

$$P_{ad} = W_c H_{ad} \qquad (7-4)$$

where W_c is the working fluid mass flow rate. Figure 7-10 thus provides for a comparison of work of compression at equal mass flow rates of the pure components. For example, hydrogen would require approximately nine times the power of the corresponding process with neon.

The comparison of Figure 7-10 deals only with the compression process, and does not consider the effect of the processes comprising the remainder of the cycle. However, the inefficiencies of the remainder of the system tend to become manifest in either higher flow rates through the compressor or higher pressure ratios. Thus, the compressor performance is probably more important than the performance of any other single component.

The relative performance of mixtures of the pure components can be determined in the following manner. For mixtures of two diatomic molecules such as nitrogen and hydrogen, the ratio of the molecular weight of the mixture to that of either nitrogen or hydrogen is multiplied by the ordinate of Figure 7-10 for the curve of the component whose molecular weight was used in the ratio. For mixtures of monatomic substances such as helium and argon, similar calculations can be made by using the curves for the monatomic gases. When mixtures of monatomic and diatomic substances are considered, the ratio of the heat capacities appearing as exponents in Equation 7-3 change and corrections must be applied in each case. In any case, it is apparent that

68

The y-axis is labeled:

$$\frac{H_{ad}}{T_{in}} = \frac{\gamma}{\gamma - 1} \frac{1545}{M} \left(Pr^{\frac{\gamma - 1}{\gamma}} - 1 \right), \ \frac{Ft}{^\circ R}$$

Curves labeled: HYDROGEN, HELIUM, NEON, NITROGEN, ARGON

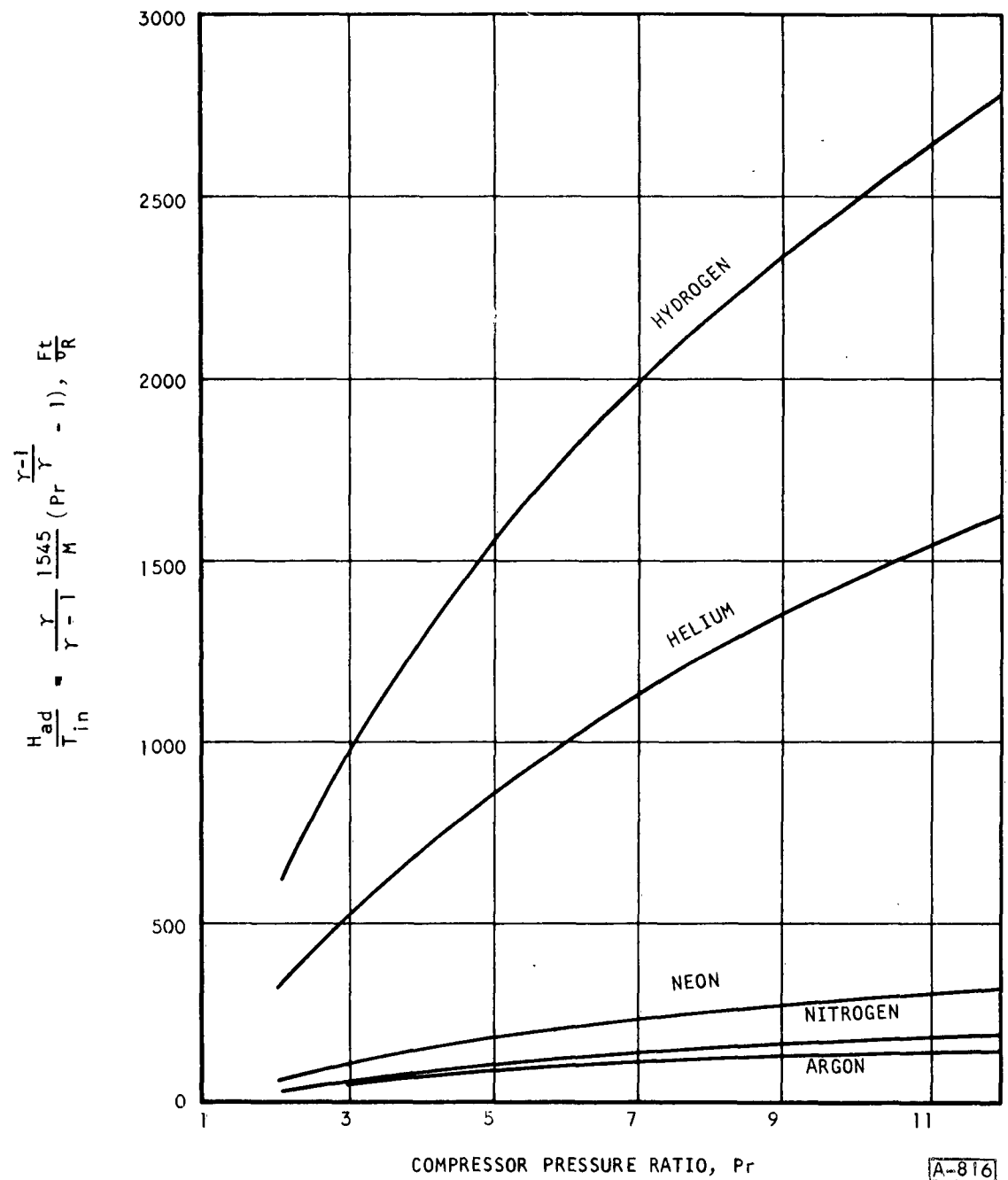COMPRESSOR PRESSURE RATIO, Pr

A-816

Figure 7-10. Effect of Molecular Weight and Specific
Heat Ratio on the Compression Progress

69

the ratio of H_{ad}/T_{in} at a particular pressure ratio Pr can be varied between the limits of the pure components comprising the mixture.
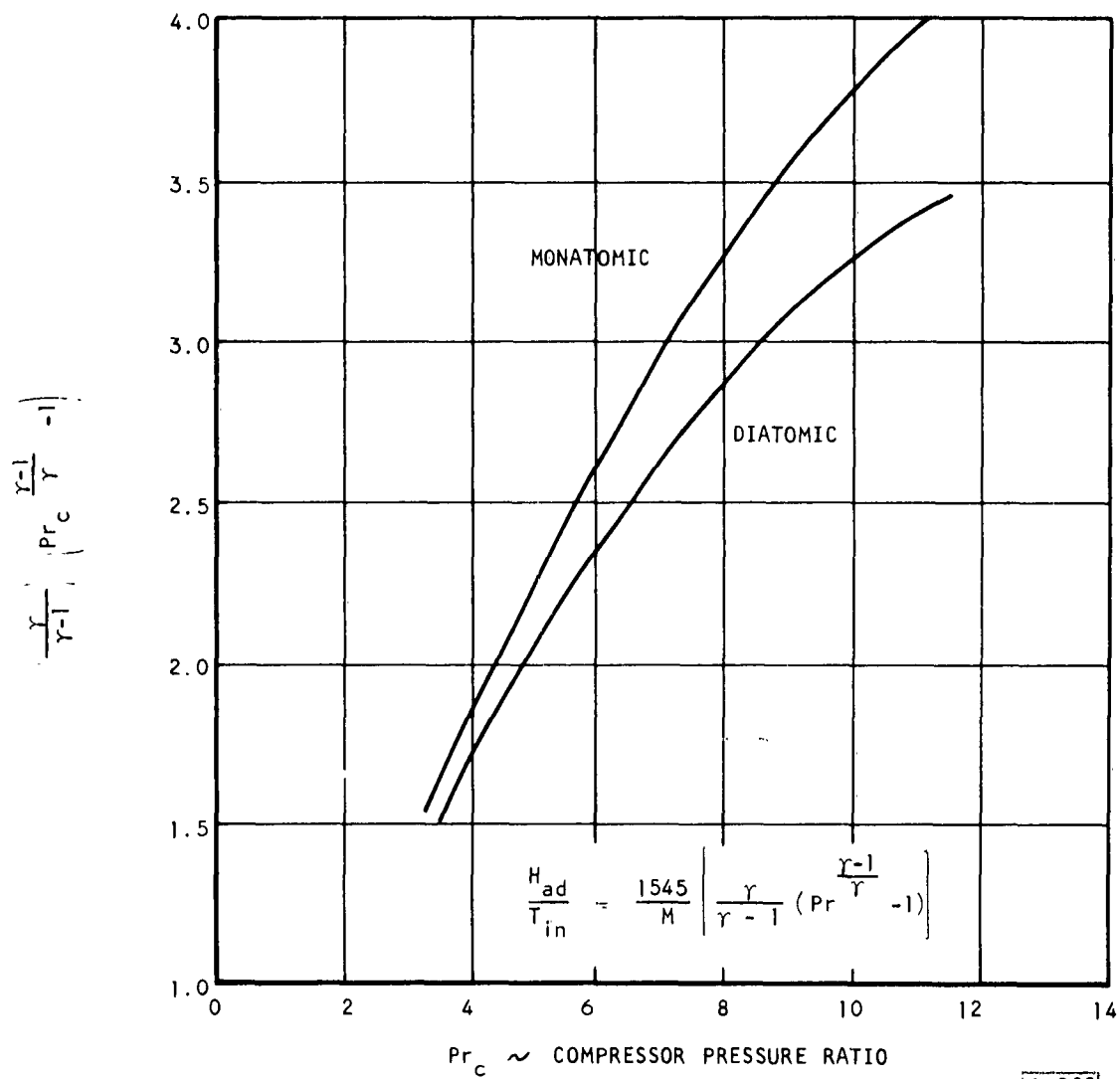
Effect of Heat Capacity Ratio

The effect of the heat capacity ratio γ in Equation 7-3 is a little less obvious than that of the molecular weight. For ideal gases, the kinetic theory of gases gives the following heat capacity ratios:

$$\text{Monatomic } \gamma = \frac{C_p}{C_v} = 1.67$$

$$\text{Diatomic } \gamma = \frac{C_p}{C_v} = 1.40$$

Figure 7-11 is a comparison of the terms of Equation 7-3 which are affected by the heat capacity ratio. This figure indicates that diatomic molecules favor lower power requirements.

It appears from Figure 7-11 that mixtures rich in diatomic molecules would be more favorable to compressor designs. This is on the supposition that the heat capacities are additive in proportion to the composition of the mixture. In cases where the inlet temperature to the compressor is relatively high and the pressure ratios considered are not too high, the additive relationship should be a good approximation.

Figure 7-11. Comparison of Effect of Heat Capacity
Ratios on Adiabatic Head

The y-axis label: $\frac{\gamma}{\gamma - 1}$, $\left(Pr_c \frac{\gamma - 1}{\gamma} - 1 \right)$

X-axis: $Pr_c \sim$ COMPRESSOR PRESSURE RATIO

Curve labels: MONATOMIC, DIATOMIC

Equation on chart:
$$\frac{H_{ad}}{T_{in}} = \frac{1545}{M} \left[\frac{\gamma}{\gamma - 1} \left(Pr^{\frac{\gamma - 1}{\gamma}} - 1 \right) \right]$$

A-809

71

SECTION 8

CONCLUSIONS AND RECOMMENDATIONS

CONCLUSIONS

The use of binary gases as cryogenic refrigerants has been shown to be not only feasible but advantageous. However, the existing data on the properties and phase behavior of mixtures are inadequate for the analyses required to select the particular mixture that gives an optimum system based on overall performance, weight, and space considerations, for a given application. The necessary data must come from experimental investigations of the type conducted during this study. Unfortunately, a major portion of the study period was spent in a preliminary literature search for existing data and on design and fabrication of the experimental apparatus, and only a brief period was available for actual measurements.

The principal binary system investigated under this contract is that of neon-argon. The slight solubility of neon in the liquid phase results in a large difference between the dew and bubble point pressures at a given temperature. This large difference makes application of neon-argon to vapor-liquid cycles of doubtful practicability. This is particularly true if constant-temperature refrigeration is required. On the other hand, the slight solubility of neon in the liquid phase results in displacement of the vapor dome of mixtures of argon and neon from that of either component. Thus, as discussed in Section 7, gas cycles can be designed to operate in the region between the two pure-component vapor domes, with possible improvement in cycle and refrigeration system component performance accruing from the use of the mixture. The time available for testing under this program did not permit PVT measurements, which are required to determine the thermodynamic properties necessary for complete refrigeration cycle analyses and for optimization of neon-argon refrigerants. Thus, comparison between systems utilizing different neon-argon mixtures and pure components could not be made. However, it was possible to examine the performance characteristics of the individual machinery components of cryogenic refrigerators, and it is concluded that judicious selection of mixtures of neon and argon, and of other binary mixtures as well, could result in improved performance and alleviation of critical design problems.

72

Mixtures of the binary systems of hydrogen and helium with the higher molecular-weight gases are expected to exhibit phase behavior similar to that of the neon-argon mixture. Thus, it appears that a wide selection of mixtures are applicable to gas cycles.

One mixture of the binary system of nitrogen-argon was investigated. A large triple-point depression (i.e., 15°K) was observed in the case of this mixture. Also, a small difference between the dew and bubble point pressures at a given temperature was observed. For example, this difference is 0.25 psi at 69°K. The development of vapor-liquid cycles utilizing this mixture and featuring a constant-temperature evaporator is particularly feasible. In cases where the difference between the dew point and bubble point pressures is large, the design of a constant-temperature evaporator becomes difficult.

Mixtures of the binary system of hydrogen and neon are expected to exhibit phase behavior similar to that of the argon-nitrogen system. Thus, mixtures of this system look particularly promising as a vapor-liquid cycle refrigerant. The principal reason for selecting argon-neon and nitrogen-argon mixtures for the measurements described in this report was that binary mixtures requiring low-temperature investigations (i.e., below 64°K) require the use of liquid hydrogen as the jacket fluid in the cryostat. AiResearch is now developing facilities for liquid hydrogen testing at Torrance, California, and lower-temperature testing will be practical in the near future.

RECOMMENDATIONS

Further experimental investigations are recommended. The consistent data obtained during the brief period of testing performed in this study provides ample evidence of the suitability of the experimental apparatus developed for this program for determining properties of binary gas mixtures in the vapor-liquid-solid transition ranges. It remains to be proved whether adequate PVT data can be obtained using this apparatus, but the quality of the data thus far obtained encourages continuation of the experimentation to include PVT measurements.

The experience gained in the course of this study and the existence of the experimental apparatus developed are factors that would expedite future investigations.

Specifically, the following investigations are recommended:

1. Mixtures of Neon-Helium and Neon-Hydrogen

Binary mixtures of the systems of neon-helium and neon-hydrogen offer promise as vapor-liquid cycle refrigerants to cover the temperature range from 4.2 to $27^{\circ}K$. For this reason, it is recommended that the phase boundaries of these systems be experimentally determined. Should the results of these investigations be favorable, additional investigations to determine the PVT properties needed for refrigeration cycle synthesis would be made.

2. Mixtures of Helium and the High-Molecular-Weight Gases

It is anticipated that helium would effect larger changes in the vapor dome of higher-molecular weight gases than neon. It is therefore recommended that a series of dew point curves be determined for mixtures of helium with argon and comparisons made with the data obtained in this program. Based on the results of this comparison, additional investigation could be directed toward a comparison of cycle performance characteristics. Thus, trends would be established to direct future work toward development of binary gas mixtures for gas cycles.

3. Detailed Analysis of the Performance of Refrigeration Components

Detailed analysis of the performance characteristics of refrigeration machinery components utilizing binary mixtures are recommended. Once binary gas mixture properties are known, the method of application of the mixture properties to specific cycle calculations will be needed. For example, performance of heat exchangers in the liquid-vapor transition range is complicated by the use of gas mixtures. In addition, actual performance tests could be conducted with existing heat exchangers, compressors and expanders. These performance tests would be invaluable as a check on analytical procedures and would furnish a guide to methods of increasing performance.

74

REFERENCES

1. M. Ruhemann, The Separation of Gases, second edition, Oxford Press, 1949.

2. Technical Note 110, National Bureau of Standards, Cryogenic Engineering Laboratory.

3. E. Hala, J. Pick, V. Fried, and O. Vilim, Vapour-Liquid Equilibrium, Pergamon Press, 1958.

4. G. M. Brown, Program, American Institute of Chemical Engineering, Houston, Texas, February 20, 1950.

5. J. G. Aston and H. L. Fink, Chemical Reviews 39, 357 (1946).

6. D. L. Katz and M. J. Rzasa, Bibliography for Physical Behavior of Hydrocarbons Under Pressure, J. W. Edwards, Ann Arbor, Michigan, 1946.

7. O. T. Bloomer and J. D. Parent, Bulletin No. 17, Institute of Gas Technology, 1952.

8. W. C. Edmister, Petroleum Refiner 28, 128 (August 1949).

9. F. Kurata and J. P. Kohn, Petroleum Process, December 1956.

10. F. G. Keyes and H. G. Burks, Journal of the American Chemical Society 50, 1100 (1928).

11. P. Z. Burbo and I. Ishkin, Physik. Z. Sowjetunion 10, 271 (1936); Physica 3, 1067 (1936).

12. G. Holst and L. Hamburger, Physik. Z. Chem. 91, 513 (1916).

13. F. Steckel, Physik. Z. Sowjetunion 8, 337 (1935).

14. B. H. Sage and W. N. Lacy, Industrial Engineering Chemistry 26, 103 (1934).

15. B. H. Sage, J. G. Schaafsma, and W. N. Lacey, ibid., 214 (1934).

16. B. H. Sage and W. H. Lacey, Transactions of the American Institute of Mining and Metallurgical Engineers 136, 136 (1940).

17. B. H. Sage, R. A. Budenholzer, and W. N. Lacey, Industrial Engineering Chemistry 32, 1262 (1940).

18. W. B. Kay, Industrial Engineering Chemistry 28, 1014 (1936).

19. W. B. Kay, ibid. 30, 459 (1938).

20. W. B. Kay, *ibid. 32*, 353 (1940).

21. W. B. Kay, *ibid. 40*, 1459 (1948).

22. J. P. Kuenen and A. L. Clark, *Commn. Phys. Lab. Leiden 150B* (1917);
    J. P. Kuenen, T. T. H. Verschoyle, and A. T. van Urk, *ibid. 161* (1922).

23. E. C. C. Baly, *Phil Mag. (5) 49*, 517 (1900).

24. T. T. H. Verschoyle, *Phil. Trans. Roy. Soc. (London) 230A*, 189 (1931).

25. F. A. Freeth and T. T. H. Verschoyle, *Proc. Roy. Soc. (London) 130A*,
    453 (1930-1931).

26. A. Fedoritenko and M. Ruhemann, *Tech. Phys. U.S.S.R. 4*, 36 (1937).

27. N. S. Torocheshnikov and V. A. Ershova, *J. Chem. Ind. (U.S.S.R.) 17*,
    No. 2, 30 (1940).

28. F. Steckel and N. Zinn, *J. Chem. Ind. (U.S.S.R.) 16*, No. 8, 24 (1939).

29. M. Ruhemann and N. Zinn, *Physik. Z. Sowjetunion 12*, 389 (1937).

30. M. Ruhemann, *Proc. Roy. Soc. (London) 171A*, 121 (1939).

31. M. Guter, D. M. Newitt, and M. Ruhemann, *Proc. Roy. Soc. (London) 176A*,
    140 (1940).

32. L. F. Stutzman and G. M. Brown, *Chemical Engineering Progress 45*, 139
    (1949).

33. B. F. Dodge and A. K. Bunbar, *Journal of the American Chemical Society 49*,
    591 (1927).

34. M. A. Rosanoff, A. B. Lamb, and F. E. Breithut, *Journal of the American
    Chemical Society 31*, 448 (1909).

35. N. S. Torocheshnikov, *Tech. Phys. U.S.S.R. 4*, 365 (1937).

36. N. S. Torocheshnikov and L. A. Levius, *J. Chem. Ind. (U.S.S.R.) 16*, No. 1,
    19 (1939).

37. A. L. Benham and D. L. Katz, *Journal of the American Institute of Chemical
    Engineers 3*, No. 1 (March 1957).

38. A. Maimoni, *Journal of the American Institute of Chemical Engineers 7*
    (1961).

39. M. R. Cines, J. T. Roach, R. J. Hogan, and C. H. Roland, *Chemical
    Engineering Progress Symposium*, Ser. 6, 49, 1 (1953).

40. H. G. Donnelly and D. L. Katz, Industrial Engineering Chemistry 46, 511 (1954).

41. R. B. Scott, Cryogenic Engineering, D. Van Nostrand Company, 1960.

42. Compendium of the Properties of Materials at Low Temperature (Phase I), WADD Technical Report 60-56, Part I.

43. F. T. Wall, Chemical Thermodynamics, W. H. Freeman and Company, 1958.

44. G. A. Cook, Argon, Helium and the Rare Gases, Volume II, Interscience Publishers, 1961 ("Phase Equilibria" by A. C. Jenkins).

45. H. M. Long and F. S. DiPaolo, Physica 24, S168 (1958).

46. R. E. Latimer, "Vapor-Liquid Equilibrium of Nitrogen-Argon-Oxygen Mixtures," American Institute of Chemical Engineering Journal 3, 75-82 (1957).

Aeronautical Systems Division, Dir/Avionics,
Reconnaissance Lab, Wright-Patterson AFB, Ohio
Rpt Nr ASD-TDR-63-339, RESEARCH ON THE APPLI-
CATION OF BINARY GAS MIXTURES TO LOW TEMPERA-
TURE COOLING SYSTEMS. Final report, May 63,
77p. incl illus., tables, 46 refs.

This report describes an investigation to de-
termine the utility of several binary gas mix-
tures as cryogenic refrigerants. The litera-
ture was searched for the existence of data
required for evaluation of the applicability
of several mixtures. An experimental appara-
tus was designed and fabricated which permitted
direct determinations of the phase boundaries
of cryogenic gas mixtures. The apparatus is
based on the dew point and bubble point method.
The general principle of this method and the
experimental apparatus and procedure for its

(over)

1. Cryogenics
2. Refrigerants
3. Coolants
4. Properties
   I. AFSC Project 4077
      Task 407703
  II. AF33(657)-8672
 III. AiResearch Manufac-
      turing Company
      Los Angeles, Calif.
  IV. Browning, C. W.
   V. SS-881-R

operation are described in detail. Experimen-
tal data were obtained for the binary systems
of neon-argon and nitrogen-argon. These data
consist of solid vapor, dew point, bubble
point, and the three-phase boundaries at a
fixed composition. Also, dew point curves
were determined for three additional neon-
argon mixtures. The possible application of
the selected mixtures, as cryogenic refriger-
ants, is discussed.